Restoration of noisy images blurred by deterministic or stochastic point spread function

by

Mehmet Bilgen

A Thesis Submitted to the

Graduate Faculty in Partial Fulfillment of the

Requirements for the Degree of

MASTER OF SCIENCE

Departments: Biomedical Engineering
Electrical Engineering and Computer Engineering
Co-majors: Biomedical Engineering
Electrical Engineering

Iowa State University
Ames, Iowa
1989

TABLE OF CONTENTS

LIST OF TABLES

LIST OF FIGURES

CHAPTER 1. INTRODUCTION

In reality, no recording is the perfect replica of the original data because of the degradation properties of the recording system or the environment. These degradations in the recording can be either systematic (spatial), such as blurring due to optical system aberrations (phase distortions), atmospheric turbulence (random variations in the refractive index of the medium between the object and the imaging system), relative motion between the object and the imaging system, diffraction limitedness and nonlinearity of the detector, or statistical, such as noise and measurement errors. For example, electron micrographs are often degraded by the spherical aberration of the electron lens and medical radiographic images are of low resolution and contrast due to the nature of the X-ray imaging systems.

Recovering a high quality image from a degraded recording is the primary purpose of the *Image Restoration*. For this purpose many restoration schemes were posed and applied extensively with some degree of success during the past.

In this research, we are primarily concerned with the restoration of images degraded by

1. Blur which might be deterministic, stochastic, known or unknown, and

2. Additive noise.

In particular, we applied inverse filter, pseudoinverse filter (least-squares), constrained least-squares filter and Wiener filter in frequency domain to estimate the original real images. A new restoration scheme, developed from constrained least-squares, was presented to restore images degraded by a stochastic blur function. The estimation accuracies of the restoration schemes were compared in terms of mean-square error. The estimation of the blur function of imaging systems from the degraded images was presented. For the purpose of illustration, the blur function was first measured from the degraded image directly, then this function was used in the restoration. Finally, application of total least squares [9] to the image restoration was discussed and the mean-square error values of one dimensional restoration results were given.

CHAPTER 2. GENERAL REVIEW OF IMAGE RESTORATION

Mathematical Model of a General Imaging System

For the convenience of analysis, any physical system is usually represented by a mathematical model if some features of the given system are known. Since capturing an image is a physical phenomenon, imaging systems can also be represented by a mathematical model. For that purpose, what a person needs is to know some properties of the given imaging system. Considering the knowledge of these properties, Jain [15] and Andrews and Hunt [2] represented a typical imaging system in a mathematical model as shown in Fig. 2.1. This model mainly consists of an image formation model, a detector/recorder model and a noise model, and can be expressed mathematically as

$$v(x,y) = g[w(x,y)] + n(x,y) \tag{2.1}$$

$$w(x,y) = \int_{-\infty}^{\infty}\int_{-\infty}^{\infty} h(x,y;p,q)u(p,q)dpdq \tag{2.2}$$

$$n(x,y) = f[g(w(x,y))]n_1(x,y) + n_2(x,y). \tag{2.3}$$

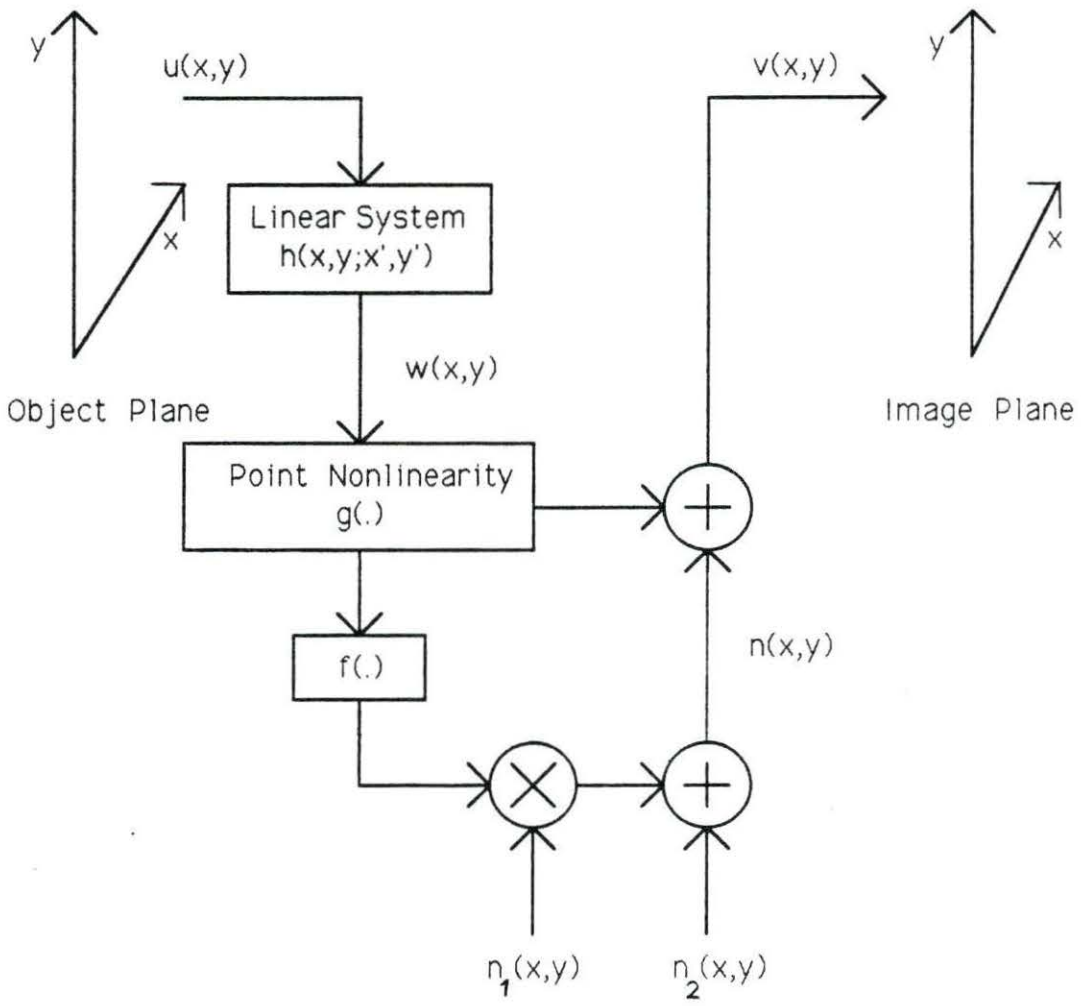

Figure 2.1: Image Recording Model

In this model, the original image $u(x,y)$ lies in the object plane and the recorded image $v(x,y)$ lies in the image plane. The continuous variable (x,y) represents the location of an image point on either plane and $u(x,y)$ (or $v(x,y)$) represents the intensity level of the image at point (x,y). $h(x,y;p,q)$ is the impulse response of the linear image formation system. In image processing terminology, the function $h(x,y;p,q)$ is called point spread function (PSF) since it is the image in the image plane due to an ideal point source at location (p,q) in the object plane. The PSF is called space invariant if the value of $h(x,y;p,q)$ depends only on the location differences, i.e.,

$$h(x,y;p,q) = h(x-p, y-q). \tag{2.4}$$

Otherwise $h(x,y;p,q)$ is called space variant. $w(x,y)$ is called a blurred image which is a superposition of the original image weighted by the PSF. The functions f and g are usually nonlinear, representing respectively sensor nonlinearity and signal-dependent noise function. The term $n(x,y)$ is the addition of image-dependent noise component $f[g(w(x,y))]n_1(x,y)$ and image independent random noise component $n_2(x,y)$. Suppose that

1. The sensors are operated in linear region (f is linear)

2. PSF is space invariant, and

3. The noise has only an image independent random component.

Eqs.(2.1)-(2.3) reduce to

$$v(x,y) = \int_{-\infty}^{\infty}\int_{-\infty}^{\infty} h(x-p, y-q)u(p,q)dpdq + n(x,y) \tag{2.5}$$

Here we used $n(x, y)$ in lieu of $n_2(x, y)$ for the simplicity of notation.

In order to restore the images by digital computers, the mathematical model of imaging system should be in the discrete variable form (difference equation). Andrews and Hunt [2] (see also [5]) showed that when sampling the continuous variable functions uniformly, the model can be reduced to discrete variable form. Moreover, if the sampled functions $h(m, n)$, $u(m, n)$, and $v(m, n)$ are periodic with a period (M, N) in spatial coordinates, the model of the imaging system can be written as [2, 5, 14, 18]:

$$v(m, n) = \sum_{i=0}^{M-1} \sum_{j=0}^{N-1} h(m - i, n - j)u(i, j) + n(m, n) \tag{2.6}$$

where the sizes of $u(m, n)$, $h(m, n)$ and $v(m, n)$ are KxL, IxJ.and MxN, respectively. The overlap in the individual periods of the convolution term in Eq. (2.6) can be avoided by choosing $M \geq K + I - 1, N \geq L + J - 1$ and padding the functions $h(m, n)$, $u(m, n)$ with zeros so that their sizes are equal to MxN. In the following pages, the sizes of the sampled functions are assumed to be MxN.

In order to write Eq. (2.6) in vector matrix form for the convenience of processing, Hunt [14] first ordered the image lexicographically by stacking the consecutive rows into a column vector, yielding

$$\mathbf{v} = \mathbf{H}\mathbf{u} + \mathbf{n} \tag{2.7}$$

where $\mathbf{v}$, $\mathbf{u}$ and $\mathbf{n}$ are vectors of dimension MNx1, KLx1 and MNx1, respectively. When the dimensions of $\mathbf{v}$ and $\mathbf{u}$ are equal, $\mathbf{H}$ becomes a block circulant matrix consisting of M^2 blocks and each block is a circulant matrix of size NxN. Again, Hunt [14] demonstrated that the circulant and block-circulant matrices can be diagonalized by one dimensional and two dimensional discrete Fourier transforms, respectively. Fol-

lowing his approach, $\mathbf{H}$ can be written as:

$$\mathbf{H} = \mathbf{W}\mathbf{D}\mathbf{W}^{-1} \tag{2.8}$$

or

$$\mathbf{D} = \mathbf{W}^{-1}\mathbf{H}\mathbf{W} \tag{2.9}$$

and

$$\mathbf{I} = \mathbf{W}\mathbf{W}^{-1} \tag{2.10}$$

where $\mathbf{D}$ is a diagonal matrix whose elements $D(k,k)$ are related to the two dimensional discrete Fourier transform (2D-DFT) of the extended point spread function $h(m,n)$ and $\mathbf{W}$ is an unitary matrix of size MNxMN whose columns are the eigenvectors of $\mathbf{H}$. Furthermore, it can be shown that the transpose of $\mathbf{H}$ is equal to

$$\mathbf{H}^{\mathrm{T}} = \mathbf{W}\mathbf{D}^{*}\mathbf{W}^{-1} \tag{2.11}$$

where $\mathbf{D}^{*}$ is the complex conjugate of $\mathbf{D}$. Using the diagonalized form of $\mathbf{H}$, Eq. (2.7) yields

$$\mathbf{v} = \mathbf{W}\mathbf{D}\mathbf{W}^{-1}\mathbf{u} + \mathbf{n}. \tag{2.12}$$

Multiplying both sides of Eq. (2.12) by $\mathbf{W}^{-1}$, we have

$$\mathbf{W}^{-1}\mathbf{v} = \mathbf{D}\mathbf{W}^{-1}\mathbf{u} + \mathbf{W}^{-1}\mathbf{n} \tag{2.13}$$

where $\mathbf{W}^{-1}\mathbf{v}$, $\mathbf{W}^{-1}\mathbf{u}$, $\mathbf{W}^{-1}\mathbf{n}$ are vectors of dimension MNx1. After rearranging the elements of these vectors and the matrix $\mathbf{D}$ into 2D-DFT representation $V(k,l)$, $U(k,l)$, $N(k,l)$ and $H(k,l)$, respectively, Eq. (2.6) can be written as

$$V(k,l) = H(k,l)U(k,l) + N(k,l) \tag{2.14}$$

where the 2D-DFT is given by [5]

$$Z(k,l) = \sum_{m=0}^{M-1} \sum_{n=0}^{N-1} z(m,n) e^{-j2\pi(\frac{km}{M}+\frac{ln}{N})} \tag{2.15}$$

for $Z = V, U, N$ or H in Eq. (2.14) and $z = v, u, n$ or h in Eq. (2.6). Similarly, the spatial domain functions can be obtained by using two dimensional inverse DFT (2D-IDFT)

$$z(m,n) = \frac{1}{MN} \sum_{k=0}^{M-1} \sum_{l=0}^{N-1} Z(k,l) e^{j2\pi(\frac{km}{M}+\frac{ln}{N})}. \tag{2.16}$$

Problems with the Image Restoration

Image restoration can be stated as a deconvolution problem or the problem of separating two convolved signals in the presence of additive noise. Examining Eq. (2.6) with known PSF uncovers two problems; the equation can be either singular at worst or ill-conditioned at best [2]. Singularity means there is no inverse transformation for a solution, in other words, the solution does not exist. On the other hand, ill-conditioned refers to the existence and uniqueness of a solution, but small changes in the recorded image **v** cause large changes in the original image **u**. From the matrix theory, condition of a matrix is determined by a condition number which is defined as the ratio of the largest eigenvalue to the smallest eigenvalue of the matrix. The larger the condition number, the higher the ill-conditioned behavior. Consequently, a solution to Eq. (2.6) can be expected to be close to the original image if the condition number of **H** is small.

A set of solutions to Eq. (2.6) can be found by using either statistical or deterministic approaches. However, the selection of the proper solution within the solution

set will be another problem. The best one from the solution set can be selected by using some optimization criteria.

When the PSF is unknown, it should be determined by either measurement or some parameter estimation methods. Of course, the uncertainity of the resulting PSF will be a new question to be answered.

In summary, the purpose of image restoration is to estimate the original image u from the degraded image v such that the estimated image $\hat{u}$ is as close to the original image u as possible, subject to a suitably chosen optimality criterion.

Previous Work in Image Restoration

Many studies in digital image processing resulted in a variety of image restoration algorithms in the past. Early image restoration methods appeared in continuous variable form. For example, a typical optical imaging system was often represented in the form of Eq. (2.5). Helstrom [12] stated the optical restoration problem as finding an estimate $\hat{u}$ that is a linear function of the degraded image v and then minimizing the mean-square error (MSE) [1] between the original image u and its estimate $\hat{u}$.

In [12], the images u, v and the noise n were assumed to be stochastic processes with known properties in the presence of deterministic PSF h. Slepian [22] approached the same problem by considering PSF h as a stochastic process with known characteristics. The foregoing two approaches yielded a two dimensional linear Wiener filter that depends on the power spectrum of the noise and the original image. In the case of stochastic PSF, the resulting Wiener filter also included the second order statistical

[1] $MSE = E[\mid u(m,n) - \hat{u}(m,n) \mid^2]$.

characteristics of the PSF. Slepian's work showed that if the MSE is small enough, at least one of the restored images is bound to be good. In addition, Helstrom [12] came up with the digital form of the Wiener filter when he considered the problem in discrete variable form (Eq. (2.6)) for digital image restorations.

The simplicity, flexibility and the power of digital computers are the main reasons for discrete image restorations. Moreover, the developments in the theory of discrete mathematics allowed the invention of different new restoration algorithms.

The first digital image restoration techniques were applied at the Jet Propulsion Laboratory (JPL) in the early 1960s in the program to land a man on the moon [2]. It was decided to land an unmanned craft which could analyze and take pictures of the surface of the moon for later work. The degradation properties of the cameras placed on the craft forced the usage of the image restoration. Consequently, JPL measured the degradation properties of the cameras before they were launched and then removed, as much as possible, the degradations from the received moon images by means of some image processing techniques.

The degradation properties of the cameras or any imaging system can basically be represented by Eq. (2.7) in vector-matrix form. The solution $\hat{\mathbf{u}}$ can be achieved as a linear function of $\mathbf{v}$ in the sense of minimum MSE (MMSE), similar to the case in continuous variable form [2, 12]. When the statistical properties of the noise $\mathbf{n}$ are unknown and even the PSF is spatially variant, a solution is still possible by means of linear least-squares. Linear least-squares requires the norm of the residual vector $\mathbf{v} - \mathbf{H}\hat{\mathbf{u}}$ to be minimized. Since there is no restriction on the values of the estimate $\hat{\mathbf{u}}$, this approach was called unconstrained restoration [18]. The unique solution was

given as the multiplication of $\mathbf{v}$ by the pseudoinverse matrix of $\mathbf{H}$ [10, 16, 23].

Mascarenhas and Pratt [17] presented computer simulations of the unconstrained restoration for underdetermined and overdetermined image observation models (i.e., the size of v is greater than that of u in overdetermined case and is less than that of u in underdetermined case). In each case, a Gaussian shaped PSF with specific variance was chosen to blur the images. Gaussian white noise with different variances was also added to the resulting blurred images. Some round-off errors were observed inherently in the computations between the original images and the estimated ones, even though there was no additive noise component $\mathbf{n}$ in Eq. (2.7). A curve was drawn to relate the condition number of matrix $\mathbf{H}$ to the changes in the variance of the Gaussian blur and the size of $\mathbf{v}$. The condition number determines the singularity of a matrix. The larger the condition number, the higher the singularity of matrix $\mathbf{H}$. For the case of high condition number of $\mathbf{H}$, Eq. (2.7) will be extermely difficult to solve and the solution becomes unstable.

One possible solution to Eq. (2.7) with singular matrices is to use Singular Value Decomposition (SVD) of $\mathbf{H}$ in the calculation of the pseudoinverse of $\mathbf{H}$ [2, 15, 18, 26]. It was observed that the singular values of the higher orders approach zero and cause the unstability of the solution (since the inverse of singular values determines the pseudoinverse of $\mathbf{H}$). In order to come up with an appropriate solution, Pratt [18] suggested a sequential algorithm in the calculation of the pseudoinverse of $\mathbf{H}$ that can be terminated before reaching the singularity of $\mathbf{H}$ which causes unstability. Unfortunately the proposed SVD image restoration was found to be computationally inefficient. In addition to that, the pseudoinverse restoration for a moderate degree of

blur was observed to be worse than the restoration for less blur. However, this trend didn't continue; the restoration for severe blur was found to be better in a subjective sense than for moderate blur.

When the PSF is spatially invariant and the associated matrix $\mathbf{H}$ is a square block circulant matrix, 2D-DFT approximation of block circulant matrices can be applied to the pseudoinverse of $\mathbf{H}$. Then the resulting filter in the frequency domain is called an inverse filter [2, 15, 18], due to being the inverse of the 2D-DFT of the PSF. However, it was stated that, in practice, the Fourier transform of the PSF drops off rapidly as a function of the distance from the origin of the frequency plane. Therefore, the inverse filter also suffered when the Fourier transform of the PSF becomes zero or close to zero.

One suggestion given [15] was to set the inverse filter to zero whenever the magnitude of the 2D-DFT of PSF is less than a suitably chosen positive threshold. Another reasonable suggestion given [2] was minimizing some linear operator on the restored image $\hat{\mathbf{u}}$, while keeping the norm of the residual vector $\mathbf{v} - \mathbf{H}\hat{\mathbf{u}}$ the same as that of the noise vector $\mathbf{n}$. This is known as the constrained least-squares method. The linear operator is allowed to have an additional control over the restoration process. It was demonstrated [2] that the resulting filter can be either Wiener filter or pseudoinverse filter depending on the selection of the linear operator.

In [14], the linear operator was chosen as the second order difference matrix because it was desirable that the solution $\hat{\mathbf{u}}$ satisfy some kind of smoothness measure and the norm of second difference of the solution was found to reflect that measure. Consequently, the lagrangian minimization method yielded a linear filter with a lagrange

multiplier as a parameter. The optimum value of this multiplier was determined iteratively [14]. The main difficulties of constrained least-squares estimation were found to be the determination of the norm of the noise term in Eq. (2.7) and the initial value of the lagrange multiplier in the iteration. However, the norm of the noise term can be estimated from the degraded image a posteriori and the convergence of the iteration can be made independent of the choice of the initial value of the lagrange multiplier.

Again, Frieden [6] discussed Backus-Gilbert method which minimizes the linear combination of the norms of the output noise term and the residual vector $\mathbf{v} - \mathbf{H}\hat{\mathbf{u}}$.

The foregoing restoration algorithms were based on linear least-squares and mean-square error methods that do not yield estimated images with positive intensity values at each pixel. However incoherent imaging systems are known as having nonnegative PSFs, inputs and outputs. Consequently, a method based on a maximum entropy concept was developed to yield nonnegative solutions [2, 15, 18, 32].

In the restoration of images by the maximum entropy method, the normalized original image is treated as a probability density function and the entropy of the normalized estimated image is maximized while keeping the norm of $\mathbf{v} - \mathbf{H}\hat{\mathbf{u}}$ and the norm of the noise term $\mathbf{n}$ equal. The experimental results showed that this method yielded sharper restorations and enhanced small points on the degraded images.

Among a variety of others, Bayesian methods are important restoration techniques when a priori information about the original image is known. In Bayesian estimation [2, 6], the a posteriori probability density function of the original image is maximized. That is to say, maximizing the probability density function of the

original image **u** given the degraded image **v** gives the maximum a posteriori estimate of **u**. If the original image **u** is assumed to be deterministic, the maximization process yields a maximum likelihood estimate. If the imaging system is linear and additive noise is a Gaussian white process, the maximum likelihood estimation reduces to the least-squares solution and the maximum a posteriori estimate reduces to the MMSE (Wiener filter) estimate for the Gaussian distributed original image **u** [27]. The Bayesian image restoration method can usually yield better results by incorporating a priori information about the original image.

In fact, the number of constraints in the foregoing restoration methods can be increased. A restoration method with more than one constraint was addressed by [31]. In [31], Youla and Webb presented some of the applications of signal reconstruction (especially tomographic image reconstruction and extrapolation of bandlimited signals) by sequential projection onto convex sets (POCS). The theory behind POCS is based on a priori construction of constraints on the solution. It was shown that if the constraints form a convex set, then a set of feasible solutions satisfying all constraints can be found iteratively. An optimal solution among all feasible solutions is then searched.

Trussell and Civanlar [25] applied the concept of POCS to the restoration of the signals. They were basically interested in determining a set of appropriate constraints, but not the optimality of the solution. As a result of this study, it was stated that the examination of the statistics of the noise can yield an important set of constraints and the fidelity of the solution increases with the number of constraints. For example, when the PSF is stochastic, finding a solution to Eq. (2.7) becomes more

difficult. Combettes and Trussell [4] recently studied this special form of problem using the POCS concept. They determined a new set of constraints by considering the statistical properties of the PSF. As expected, the diameter of feasible solution set was increased due to the uncertainity of the PSF.

The ill-conditioned problem was reformulated by Ross [20], and called regularization, so that a solution which is not only less sensitive to the small perturbations in the data $\mathbf{v}$ but also close to the original data $\mathbf{u}$ can be found. However, the regularization process yields a solution as a function of a variable, called the regularization parameter. Ross introduced an iterative fast algorithm for obtaining a feasible solution and established a criterion for determining an optimum value for the regularization parameter.

Another digital image restoration method which has received much attention in the literature is Kalman Filtering (KF). Well known as a great success in one dimensional signal processing, KF is basically known as optimal linear estimator minimizing the MSE. Nevertheless KF is different from the Wiener filter in the sense of estimating the data recursively after the new observations.

In 1977, Woods and Radevan [30] (see also Biemond [3]) extended the conventional one dimensional KF to two dimensions. Requiring high dimensional matrices, the direct extension of KF was found to be computationally very inefficient. In order to improve the computational efficiency, the authors introduced a Kalman strip processor that updates one line in the image at a time, and a Kalman scalar processor that updates one point in the image at a time. It was shown that the proposed techniques are computationally attractive and applicable to the nonstationary images

degraded by space variant PSFs. It was hoped that the nonlinear models with space variant PSFs could be treated using similar techniques.

Little work on the restoration of images degraded by a stochastic PSF in the presence of additive noise can be found in the literature. As we mentioned at the beginning, Slepian [22] dealt with the solution of Eq. (2.5) when the PSF is stochastic. His approach yielded the Wiener filter as a function of the second order statistics of the PSF. Later Ward and Saleh [28] developed two iterative nonlinear methods based on modifications of the Wiener filter and the minimum variance unbiased estimation techniques. The methods were both nonlinear and iterative because the unavailability of the correlation matrix of the object image used in Wiener filter requires iterative estimation from the degraded image. The proposed methods were tested on one dimensional signals assuming the PSF and additive noise were uncorrelated. As a result, the minimum variance unbiased estimation, derived from maximizing the probability function, was observed to yield better results.

On the other hand, two papers dealing with the restoration of stochastically degraded images recently appeared. In the first paper, Guan and Ward [11] extended the modified iterative Wiener filter, developed earlier by Ward and Saleh [28], into two dimensional parametric form. The calculations were carried out in the frequency domain by using block circulant matrix approximation of the mean value of a stochastic PSF matrix. The restoration results of the modified Wiener filter in an iterative fashion were observed to be both inexpensive and better than those of the linear Wiener filter and the Backus-Gilbert technique in the sense of MSE.

Ward and Saleh [29] modified the Backus-Gilbert technique for restoration of im-

ages degraded by a stochastic PSF. The developed method was based on the weighted superposition of a small number of shifted versions of the distorted image. With this property, the resulting filter was linear and similar to the finite impulse response filter. The weights in the superposition were determined by optimizing a combined measure of the resolution and noise. Compared with both the Wiener filter requiring the knowledge of the ensemble average power spectrum of the image, and the minimum variance unbiased estimator, requiring extensive computations, the proposed method yielded better restored images.

Stockham et al. [24] addressed the problem of deconvolving two signals when both are unknown. This approach was called blind deconvolution. Here the extent of one of the signals was assumed to be considerably smaller than the other. For example, in the restoration of conventional acoustic recordings, the waveform span of the acoustic signal is longer than the extent of the impulse response of the recording mechanism. The authors developed homomorphic filtering and power spectrum estimation schemes to recover the original speech. For the purpose of illustration, unknown blurs from the degraded images were eliminated by using the theoretical results developed for one dimensional restoration. For images of large dynamic range, the homomorphic filtering approach was observed to provide smoother results compared with the power spectrum estimation method.

Finally in terms of application areas, current literature [2, 4, 15, 31] reveals that digital image restoration methods are extensively used in medicine (diagnostic X-rays, cell biology, anatomy, physiology); in physics (plasma diagnostics, ultrahigh- pressure shockwaves, solid state phenomena); in nondestructive testing (visual quality control

inspection, acoustic holography); in weather forecasting (observation of visible cloud features from weather satellites); in resource exploration (two dimensional seismic signal processing); and so on.

Statement of the Problem

Digital image restoration is mainly concerned with recovering the original image, given the degraded image and some knowledge about the properties of the degradations. In this thesis, we focus on images that are modeled by a linear shift invariant system, namely

$$\mathbf{v} = \mathbf{H}\mathbf{u} + \mathbf{n} \tag{2.17}$$

where $\mathbf{v}$ is the observed or recorded image, $\mathbf{u}$ is the original image, $\mathbf{n}$ is Gaussian noise vector with zero mean and uncorrelated elements and $\mathbf{H}$ is a block circulant PSF matrix.

Consequently, by knowing $\mathbf{v}$ and the statistical characteristic of $\mathbf{n}$, our primary goal is to restore $\mathbf{u}$ for the following cases:

a) Deterministic PSF matrix which is known.

b) Stochastic PSF matrix with known mean and variance.

c) Deterministic PSF matrix which is unknown.

In the following sections, the above cases will be considered separately. In considering cases described by (a) and (b) above, various existing algorithms will be applied to restore the real images degraded by computer generated deterministic or stochastic

PSF and additive Gaussian white noise. However, in (c) the unknown PSF will be determined from a systematically degraded image.

CHAPTER 3. METHODS AND RESULTS OF DIGITAL IMAGE RESTORATION

In the first section, we introduce the digitization procedure and give the statistical properties of the test images to be used in computer simulations.

In the second section, we primarily study the performance of several existing image restoration techniques for images blurred by the known deterministic PSF and corrupted by additive signal-independent noise. The restoration results for each method were given for the purpose of comparison.

In the third section, we propose a new method under the framework of the constrained least-squares technique to restore images blurred by the stochastic PSF and corrupted by additive signal-independent noise. The proposed method requires the signal-to-noise ratio of the degraded image to be less than an a priori known value. If this condition is satisfied, the simulation results show that our method outperforms other existing techniques in terms of average mean-square error (AMSE)[1]. In the fourth section, we attempt to estimate the PSF of imaging systems from the degraded images before a specific restoration technique is applied.

[1] $AMSE = \frac{1}{MN} \sum_{m=0}^{K-1} \sum_{n=0}^{L-1} (u(m,n) - \hat{u}(m,n))^2$.

Figure 3.1: Original images: a) Picture of a girl, b) X-ray film of tibia

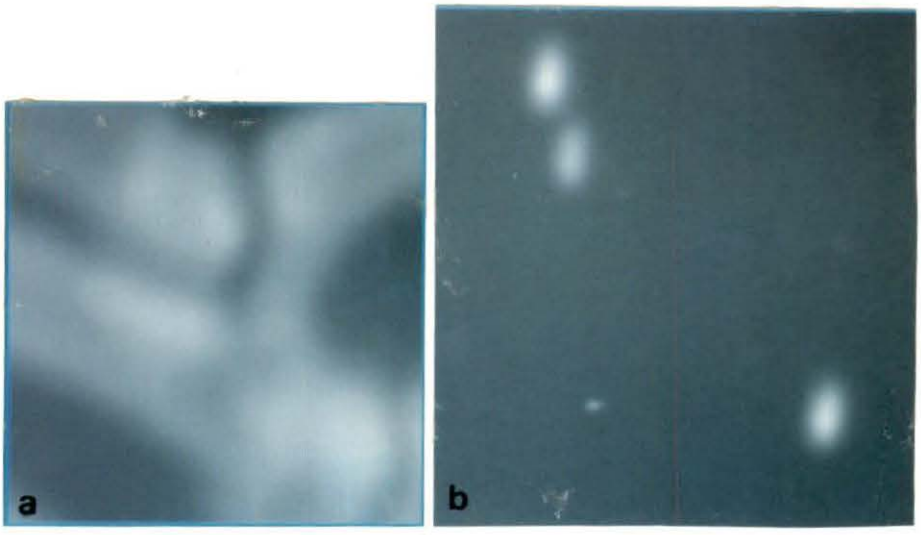

Figure 3.2: Systematically blurred images: a) X-ray film of phalanges, b) Blurred dots to measure the PSF of X-ray imaging system

Description of Test Images in Computer Simulations

Fig. 3.1 shows a standard picture of a girl and an X-ray film of a tibia representing the original images for the computer simulations. The simulations were performed in a Hewlett-Packard HP 9000/360 series computer. Fig. 3.2 shows systematically degraded X-ray film of phalanges and the dots to be used for the determination of the PSF of the imaging system. These pictures were digitized into the images of 100x100 pixels with 8 bit intensity quantization by minimizing the tradeoff between the resolution and the size.

Fig. 3.1a, standard test image used often in the literature, has an average gray level of 178.180, a variance of 2832.627 and an energy ($\| \mathbf{u} \|^2$) of 3.458E+8. Fig. 3.1b has an average of 131.798, a variance of 7001.048 and an energy of 2.437E+8.

In order to blur the original images in Fig. 3.1, a symmetric Gaussian shaped function $h(m,n)$ was selected as the PSF:

$$h(m,n) = K e^{-\frac{m^2+n^2}{2\sigma^2}} \tag{3.1}$$

where K is a scaling factor which normalizes $h(m,n)$, i.e $\sum_m \sum_n h(m,n) = 1$. The program, MAIN1, given in Appendix, was used to perform the degradations due to blur and signal-independent additive noise. The routines (Eq. (2.6) in the spatial domain and Eq. (2.14) in the frequency domain) were implemented by calling 2D-DFT subroutine FFT and Gaussian random noise subroutine NORMAL. Fig. 3.3 represents the blurred forms of images in Fig. 3.1 when the chosen PSF is of size 19x19 with variance 4.0. With this selection of PSF, the size of convolution in Eq. (2.6) is less than 128x128 ($2^7 = 128$) so that the wraparound effects due to the convolution process

Figure 3.3: Images blurred by Gaussian shaped PSF of variance 4.0

are prevented. Fig. 3.4 is the noise added form of Fig. 3.3. Here the noise of variance 100 is generated using the subroutine NORMAL that creates uncorrelated, zero mean Gaussian numbers with unity variance. Corresponding signal-to-noise ratios (SNR)[2] of Fig.3.4a and Fig.3.4b are 14.42 db and 18.45 db, respectively. In the following sections, Fig. 3.4 will be the degraded image to which the restoration schemes will be applied.

Restoration of Noisy Images Degraded by Deterministic PSF

In this section, we present the results of the restored images based on inverse filtering, Wiener filtering and constraint least-squares filtering. We also use AMSE as an objective quality measure to compare the performance of the aforementioned

[2]SNR is defined as the ratio of the variance of the original image to that of the signal-independent noise.

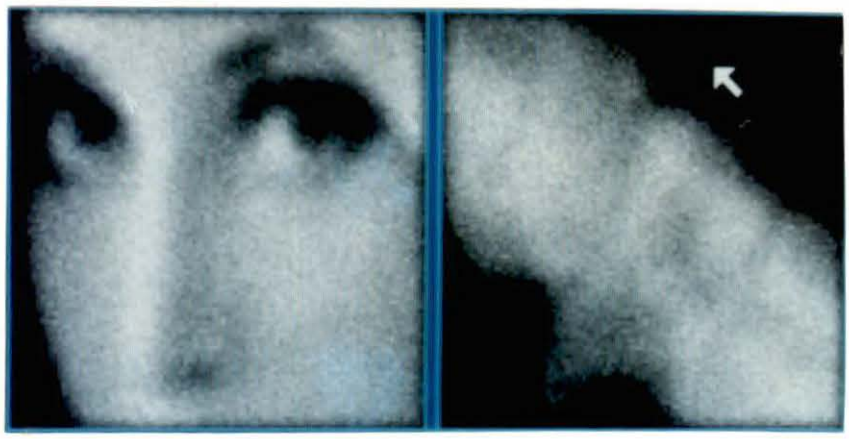

Figure 3.4: Noisy form of blurred images in Fig. 3.3. Noise variance is 100

restoration methods.

Inverse Filtering

Based on Eq. (2.7), minimizing $\| \mathbf{v} - \mathbf{H}\mathbf{u} \|^2$ with respect to $\mathbf{u}$ in the least-square sense yields a solution given by [10, 16, 23]

$$\hat{\mathbf{u}} = (\mathbf{H}^{\mathrm{T}}\mathbf{H})^{-1}\mathbf{H}^{\mathrm{T}}\mathbf{v}. \tag{3.2}$$

When the PSF matrix $\mathbf{H}$ is a square matrix and nonsingular, Eq. (3.2) reduces to

$$\hat{\mathbf{u}} = \mathbf{H}^{-1}\mathbf{v} \tag{3.3}$$

Again, approximating the block circulant matrix $\mathbf{H}$ by the 2D-DFT, Eq. (3.3) will be

$$\hat{U}(k,l) = \frac{V(k,l)}{H(k,l)}$$

where $\hat{U}(k,l)$, $V(k,l)$ and $H(k,l)$ are the 2D-DFTs of the estimated image $u(m,n)$, degraded image $v(m,n)$ and the PSF $h(m,n)$, respectively. Program MAIN2 in Appendix implements the inverse filtering routine in the frequency domain by setting $\hat{U}(k,l) = 0$ whenever $\mid H(k,l) \mid^2$ is a less-than-suitably chosen quantity to eliminate excessively large error when $H(k,l)$ is close to zero. Fig. 3.5 represents the restored form of images in Fig. 3.4. It is clear that the inverse filtering routine recovers much of the details by causing additional effects along the edges.

Wiener Filtering

Assume that the restored image is a linear operation on the degraded image, i.e., $\hat{\mathbf{u}} = \hat{\mathbf{H}}\mathbf{v}$, and the original image and signal-independent noise are the samples of two dimensional random processes with zero mean and known covariance matrices. Minimization of mean square error $E[\mid \mathbf{u} - \hat{\mathbf{u}} \mid^2]$ yields the Wiener filter [2, 15, 18]. For a general nonlinear image model with space-variant blur, the linear operator can be given by [18]

$$\hat{\mathbf{H}} = \mathbf{C_{uv}}(\mathbf{C_{vv}})^{-1} \tag{3.4}$$

where $\mathbf{C_{uv}}$ is the cross covariance matrix between the original and degraded images and $\mathbf{C_{vv}}$ is the covariance matrix of the degraded image. If the imaging system is the linear model given by Eq. (2.7), the linear function reduces to [2, 15, 18]

$$\hat{\mathbf{H}} = \mathbf{C_u}\mathbf{H}^{\mathrm{T}}(\mathbf{H}\mathbf{C_u}\mathbf{H}^{\mathrm{T}} + \mathbf{C_n})^{-1} \tag{3.5}$$

where $\mathbf{C_u}$ and $\mathbf{C_n}$ are the covariance matrices of the original image and noise proccess respectively. In order to obtain a rapid Fourier computation, the circulant approximation to $\mathbf{C_u}$, $\mathbf{C_n}$ and $\mathbf{H}$ is assumed [2]. Then Eq. (3.5) can be expressed in the

frequency domain as

$$\hat{H}(k,l) = \frac{H^*(k,l)}{\mid H(k,l) \mid^2 + \frac{C_n(k,l)}{C_u(k,l)}} \tag{3.6}$$

where $C_u(k,l)$ and $C_u(k,l)$ are the power spectra of the original image and the noise, respectively.

Quite often, original images have nonzero means. If the original image has non-stationary mean, we cannot use the circulant approximation, and Eq.(3.6) can not be applied. However, if the original image has stationary mean, $\mathbf{m}$, then the restored image $\hat{U}(k,l)$ in the frequency domain is given by [15]

$$\hat{U}(k,l) = \hat{H}(k,l)(V(k,l) - H(k,l)M(k,l)) + M(k,l) \tag{3.7}$$

where $M(k,l)$ is the 2D-DFT of the mean of the original image, $\mathbf{m}$. To obtain the final restored images, Eq.(3.6) or Eq.(3.7) is thus computed by the 2D-IDFT.

Fig. 3.6 represents the images in Fig. 3.4 restored by the Wiener filter routine in program MAIN2 when the images are assumed to have zero mean. However, our experience shows that Wiener filter for nonzero mean images (Eq. 3.7) can yield smoother images with reduced dynamic range and increased AMSE.

Constrained-Least Square Filter

The constrained least-square filter is based on the minimization of a linear function of the original image such that the norm of the resulting residual vector is equal to that of the noise vector [14]. The filter can be constructed according to:

Minimize $\| \mathbf{Qu} \|^2$

Subject to $\| \mathbf{v} - \mathbf{Hu} \|^2 = \| \mathbf{n} \|^2$

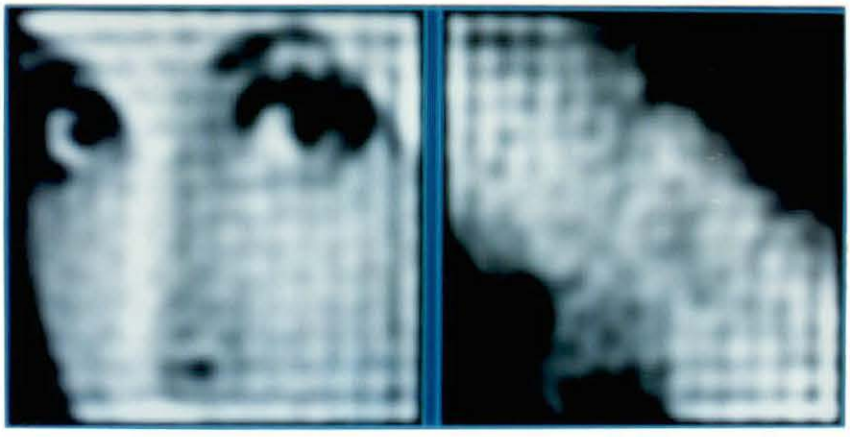

Figure 3.5: Restoration of Fig.3.4 by Inverse Filter, Threshold=0.06: (a) $AMSE = 534.831$, (b) $AMSE = 355.427$

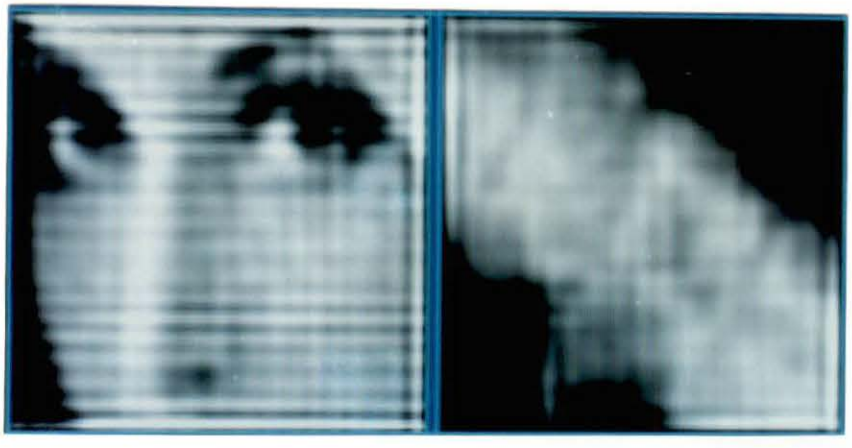

Figure 3.6: Restoration of Fig.3.4 by Wiener Filter, Noise variance is 100: (a) $AMSE = 764.550$, (b) $AMSE = 229.480$

where $\mathbf{Q}$ is a linear operator. Using the lagrange optimization method, the estimate can be given by [14]

$$\hat{\mathbf{u}} = (\mathbf{H}^{\mathrm{T}}\mathbf{H} + \gamma\mathbf{Q}^{\mathrm{T}}\mathbf{Q})^{-1}\mathbf{H}^{\mathrm{T}}\mathbf{v} \tag{3.8}$$

where γ is the inverse of the lagrangian parameter to be determined to satisfy the constraint and $\| \mathbf{n} \|$ is the norm of the noise vector which may be known a priori or which can be estimated from the smooth regions of the degraded image. Under the circular approximations, Eq. (3.8) can be written in frequency domain as [14]

$$\hat{U}(k,l) = \frac{H^{*}(k,l)V(k,l)}{\mid H(k,l) \mid^2 + \gamma \mid Q(k,l) \mid^2} \,. \tag{3.9}$$

Hereafter the residual vector, $\mathbf{r} = \mathbf{v} - \mathbf{H}\hat{\mathbf{u}}$, in the frequency domain can be written as

$$R(k,l) = \frac{\gamma \mid Q(k,l) \mid^2 V(k,l)}{\mid H(k,l) \mid^2 + \gamma \mid Q(k,l) \mid^2} \tag{3.10}$$

where $R(k,l)$ is the 2D-DFT of the residual $r(m,n)$. If the norm of the residual vector $\mathbf{r}$ is equal to that of the noise vector $\mathbf{n}$, then $\hat{\mathbf{u}} = \mathbf{u}$. In fact, the norm of the residual can be calculated in the frequency domain by means of Parseval's theorem as

$$\| \mathbf{r} \|^2 = \sum_{m=0}^{M-1} \sum_{n=0}^{N-1} \mid r(m,n) \mid^2 = \frac{1}{MN} \sum_{k=0}^{M-1} \sum_{l=0}^{N-1} \mid R(k,l) \mid^2 \,. \tag{3.11}$$

Moreover, it was shown [14] that $\| \mathbf{r} \|^2$ is monotonically increasing as a function of γ. Hence, there is only one value of γ that satisfies the constraint. This optimal value of γ can be found by using optimization techniques such as the Newton-Raphson method [7]. The Newton-Raphson method is an iterative process of finding a root of a function $f(x)$, starting from an initial estimate. The procedure can be summarized as [7]

START initial guess x_1

IF $f'(x_1) \neq 0.0$ THEN $x_2 = x_1 - f(x_1)/f'(x_1)$

DO WHILE $\mid x_2 - x_1 \mid \geq$ Tolerance Value 1, OR

$\mid f(x_2) \mid \geq$ Tolerance Value 2, AND $f'(x_1) \neq 0.0$

SET $x_2 = x1 - f(x_1)/f'(x_1)$

SET $x_2 = x_1$

ENDDO

Application of the Newton-Raphson method requires the derivative of the function $f(\gamma) = \| \mathbf{r} \|^2 - \| \mathbf{n} \|^2$. From Eqs. (3.10)-(3.11), the derivative of $f(\gamma)$ with respect to γ can be given by

$$f'(\gamma) = \frac{1}{MN} \sum_{k=0}^{M-1} \sum_{l=0}^{N-1} \frac{\gamma \mid Q(k,l) \mid^2}{(\mid H(k,l) \mid^2 + \gamma \mid Q(k,l) \mid^2)^3}. \tag{3.12}$$

As a result of foregoing explanations, the constrained least-squares image restoration is implemented in the discrete frequency domain. Also, examining Eq. (3.9) reveals that the selection of the linear function $\mathbf{Q}$ results in different forms of filters as shown below.

1. $\mathbf{Q} = \mathbf{0}$ or $\gamma = 0$ results in the inverse filter.

2. $\mathbf{Q} = \mathbf{C_u^{-1/2} C_n^{1/2}}$ minimizes the effective noise to signal ratio of the estimated image and yields the Fourier Wiener filter given by Eq. (3.5).

3. $\mathbf{Q} = \mathbf{I}$ minimizes the energy of the restored image yielding the pseudoinverse filter.

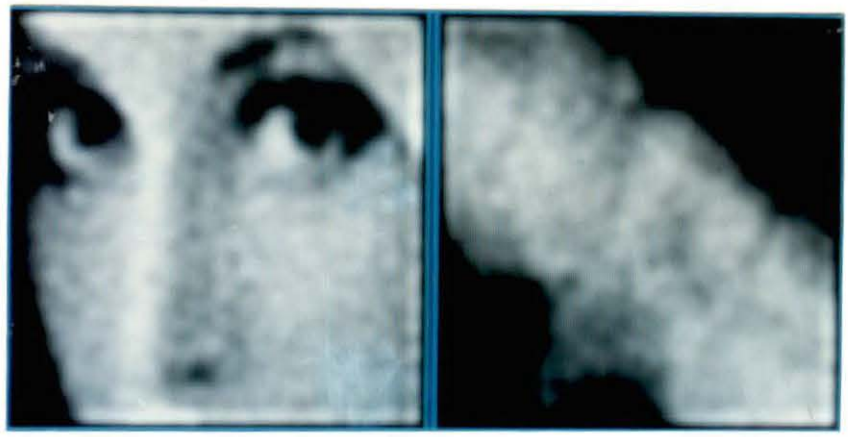

Figure 3.7: Restoration of Fig. 3.4 by Pseudoinverse Filter: (a) $AMSE = 556.083$, $\gamma = 5.56E-2$ at 4 iterations, (b) $AMSE = 424.093$, $\gamma = 8.71E-2$ at 5 iterations

4. When **Q** represents the second order derivative operator [14] the resulting estimate satisfies the smoothness measure.

At this point, we are interested in implementing only the last two forms, since we have already introduced the results of the first two. Fig. 3.7 and Fig. 3.8 represent the images in Fig. 3.4 restored by a pseudoinverse filter and a second order derivative filter, respectively. MAIN2 yields Fig. 3.7 when $\| \mathbf{n} \|^2$ is 3000000 with tolerance 1000 and the initial value of γ is 0.01 with tolerance 1.0E-6. Similarly, Fig. 3.8a and Fig. 3.8b are obtained when $\| \mathbf{n} \|^2$ is 2300000 and 1500000, respectively, with tolerance 1000 and the initial value of γ is 0.0001 with tolerance 1.0E-6. As expected, the second order derivative operator routine yielded smoother results than the pseudoinverse filter.

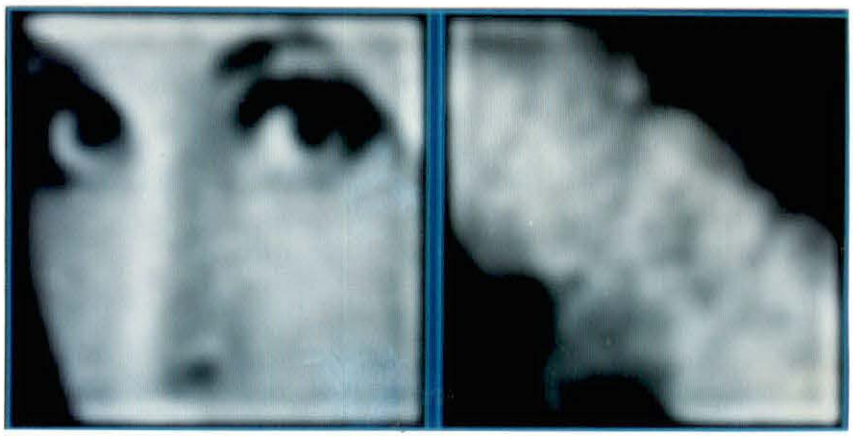

Figure 3.8: Restoration of Fig. 3.4 by Second Order Difference Filter: (a) $AMSE = 499.829$, $\gamma = 0.423$ at 6 iterations, (b) $AMSE = 265.089$, $\gamma = 0.382$ at 7 iterations

Restoration of Noisy Images Degraded by Stochastic PSF

PSFs of real imaging systems usually have uncertainities due to the environmental or the systematic effects. For example, X-ray imaging systems, scanning microscopes and microdensiometers are known to have blur functions with uncertanities [4]. If the uncertainity in the PSF matrix $\mathbf{H}$ is additive and confined to the size of the PSF, the linear shift invariant system in the presence of additive noise can be written as

$$\mathbf{v} = (\bar{\mathbf{H}} + \mathbf{N}_1)\mathbf{u} + \mathbf{n}_2 \tag{3.13}$$

or

$$\mathbf{v} = \bar{\mathbf{H}}\mathbf{u} + \mathbf{n} \tag{3.14}$$

$$\mathbf{n} = \mathbf{N_1 u} + \mathbf{n_2} \tag{3.15}$$

where the matrix $\bar{\mathbf{H}}$ is the mean of the stochastic PSF matrix $\mathbf{H}$, and the matrix $\mathbf{N_1}$ represents the variations about its mean $\bar{\mathbf{H}}$. The following assumptions are made:

1. The matrix $\mathbf{N_1}$ consists of uncorrelated elements with variance σ_1^2.

2. The signal-independent additive noise vector $\mathbf{n_2}$ has uncorrelated elements with variance σ_2^2.

3. The elements of $\mathbf{N_1}$ and $\mathbf{n_2}$ are uncorrelated.

In the following, we study the Wiener filter developed in [28] and propose a new technique based on the conventional constrained-least squares filter for this restoration problem. Also, for the purpose of performance comparison, the conventional Wiener filter (Eq. (3.7)) and constrained least squares filter (Eq. (3.9)) were implemented. Simulations show that our algorithm can yield better results in the sense of AMSE.

Wiener Filtering

Ward and Saleh [28] proposed a technique for restoration of the images degraded by a stochastic PSF based on the Slepian's work [22], yielding a linear function

$$\hat{\mathbf{H}} = \mathbf{C_u H^T}(\mathbf{H C_u H^T} + E[\mathbf{C_n}])^{-1} \tag{3.16}$$

and

$$\mathbf{C_n} = E[\mathbf{n n^T}] = E[(\mathbf{N_1 u} + \mathbf{n_2})(\mathbf{N_1 u} + \mathbf{n_2})^{\mathbf{T}}] \tag{3.17}$$

Figure 3.9: Stochastically blurred images, $\sigma_1^2 = 0.0025$

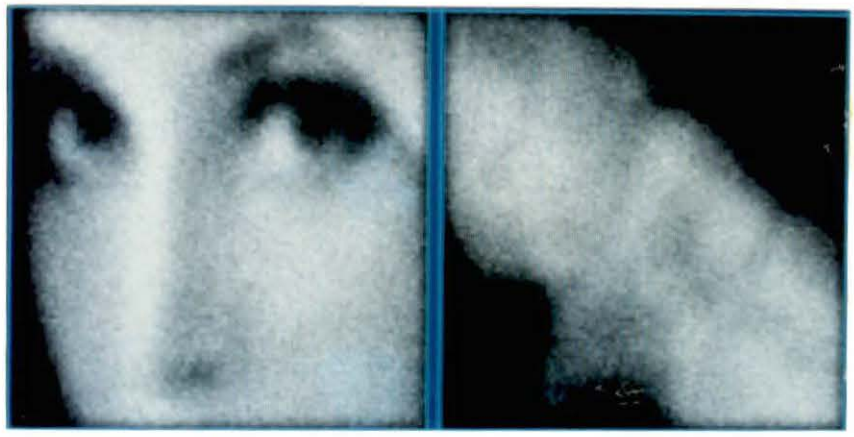

Figure 3.10: Noisy form of stochastically blurred images, $\sigma_2^2 = 100$

where the expectation in Eq. (3.16) is over $\mathbf{u}$ and the expectation in Eq. (3.17) is over $\mathbf{N_1}$ and $\mathbf{n_2}$. Eq. (3.16) is similar to the conventional Wiener filter in Eq. (3.5), except for the expectation operation, $E[\mathbf{C_n}]$. Since we assumed that the uncertainity in the PSF is uncorrelated with original image and signal-independent additive noise, Eq. (3.16) reduces to [28]

$$[\mathbf{C_n}]_{ij} = (M-i)(N-j)\sigma_1^2[\mathbf{C_u}]_{ij} + \sigma_2^2$$

where σ_1^2 and σ_2^2 are the variances of uncertainity in the PSF and additive noise, respectively. Using the 2D-DFT approximation of the block circulant matrices, Eq. 3.16 can be written as [11]

$$\hat{H}(k,l) = \frac{\bar{H}^*(k,l)}{\mid \bar{H}(k,l) \mid^2 + IJ\sigma_1^2 + \frac{C_{n_2}(k,l)}{C_u(k,l)}} \tag{3.18}$$

where I, J is the size of the PSF and $C_u(k,l)$ and $C_n(k,l)$ are the power spectra of the original image and the noise, repectively. Since the images in real life have nonzero mean, the mean of the original image $M(k,l)$ in frequency domain should be included in the final form

$$\hat{U}(k,l) = \hat{H}(k,l)(V(k,l) - H(k,l)M(k,l)) + M(k,l).$$

Experimental Results

We consider $\bar{\mathbf{H}}$ is a block circulant matrix representation of a Gaussian function with variance 4.0 and size $I = J = 19$, $\mathbf{N_1}$ is a block circulant matrix representation of a two dimensional Gaussian white noise process with elements of variance $\sigma_1^2 = 0.00000625$, and $\mathbf{n_2}$ is the additive Gaussian noise vector whose elements are

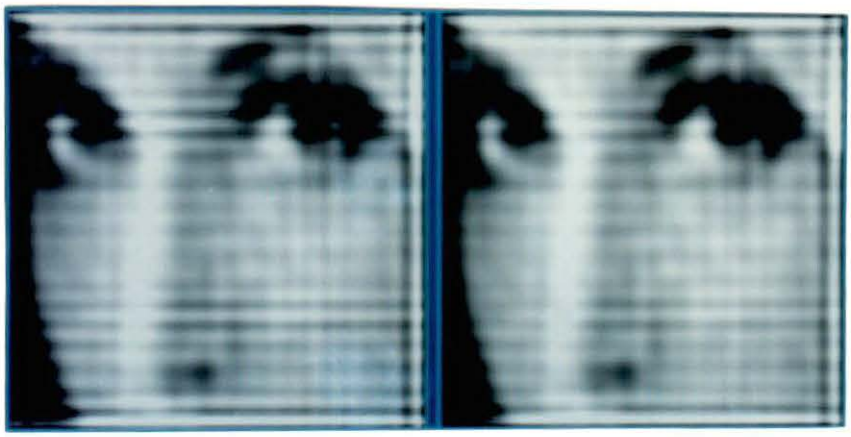

Figure 3.11: Restoration of Fig. 3.10a, $\sigma_1^2 = 0.00000625$ and $\sigma_2^2 = 100$: (a) Conventional Wiener filter, $AMSE = 885.066$, (b) Modified Wiener filter, $AMSE = 636.280$

uncorreleted having variance $\sigma_2^2 = 100$. Program MAIN1 implements the foregoing conditions on the original images in Fig. 3.1. Fig. 3.9 shows the images blurred by stochastic PSF and Fig. 3.10 shows the noisy form of Fig. 3.9. Hence, in the following pages, Fig. 3.10 represents the degraded images to be restored.

We first used the conventional Wiener filter (Eq. (3.6)) that yielded Fig. 3.11a and Fig. 3.12a as the restored images in Fig. 3.10. When Eq. (3.18) is used, Fig. 3.11b and Fig. 3.12b result. Compared with the conventional Wiener filter results, the modified Wiener filter results are more clear and smoother with lower AMSE values.

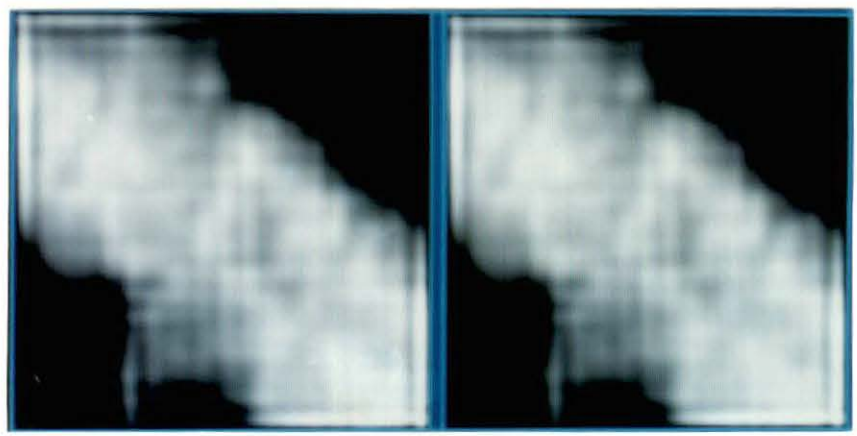

Figure 3.12: Restoration of Fig. 3.10b, $\sigma_1^2 = 0.00000625$ and $\sigma_2^2 = 100$: (a) Conventional Wiener filter, $AMSE = 276.406$; (b) Modified Wiener filter, $AMSE = 259.390$

The Proposed Approach

First of all, we reviewed the method by Combettes and Trussell [4], which was related to our work. The basic idea behind their work is to construct a closed convex set based on the statistics of the residual signal and then apply the projections onto convex sets(POCS) method [31] to obtain a feasible restored image.

Suppose that the statistics of the PSF matrix $\mathbf{H}$ are known, the residual vector can be defined by $\mathbf{v} - \mathbf{H}\hat{\mathbf{u}}$ where $\hat{\mathbf{u}}$ represents the restored image. It is clear that if the original image is perfectly recovered $\hat{\mathbf{u}} = \mathbf{u}$, then $\mathbf{v} - \mathbf{H}\hat{\mathbf{u}} = \mathbf{n_2}$. Although $\mathbf{n_2}$ is unknown, its statistics are generally available from the flat regions of the degraded images. Therefore, it is reasonable to have the sample statistics of the residual vector in agreement with those of the $\mathbf{n_2}$.

Assuming the knowledge of $\bar{\mathbf{H}}$ and the second order characteristics of uncertainity in the PSF, Combettes and Trussell [4] formed a constraint based on the residual vector

$$\mathbf{r} = \mathbf{v} - \bar{\mathbf{H}}\hat{\mathbf{u}}. \tag{3.19}$$

When the estimate $\hat{\mathbf{u}}$ is equal to the original image $\mathbf{u}$, the residual becomes

$$\mathbf{r} = \mathbf{N_1 u} + \mathbf{n_2}; \tag{3.20}$$

thus

$$\| \mathbf{r} \|^2 = E[(\mathbf{N_1 u} + \mathbf{n_2})^{\mathrm{T}}(\mathbf{N_1 u} + \mathbf{n_2})]. \tag{3.21}$$

Since the original image $\mathbf{u}$, the uncertainity $\mathbf{N_1}$ and additive noise $\mathbf{n_2}$ are assumed to be uncorrelated,

$$\| \mathbf{r} \|^2 = E[\mathbf{n_2}^{\mathrm{T}}\mathbf{n_2}] + E[\| \mathbf{N_1 u} \|^2]. \tag{3.22}$$

From the inequality

$$E[\| \mathbf{N_1 u} \|^2] \leq \| \mathbf{u} \|^2 \, E[\| \mathbf{N_1} \|^2] \tag{3.23}$$

it can be shown [4] that

$$\| \mathbf{r} \|^2 \leq E[\| \mathbf{n_2} \|^2] + \beta \| \mathbf{u} \|^2 \tag{3.24}$$

where

$$\beta = E[\| \mathbf{N_1} \|^2] = \sum_{i=0}^{I-1} \sum_{j=0}^{J-1} E[\, | \mathbf{N_1}(i,j) |^2]. \tag{3.25}$$

Therefore, the conventional constrained least-squares problem is modified to

Minimize $\| \mathbf{Q}\hat{\mathbf{u}} \|^2$

Subject to $\| \mathbf{v} - \bar{\mathbf{H}}\hat{\mathbf{u}} \|^2 = E[\| \mathbf{n_2} \|^2] + \beta \| \hat{\mathbf{u}} \|^2$

where $\mathbf{Q}$ is a linear operator. Using the method of lagrange multipliers and block circulant approximation of PSF matrix $\bar{\mathbf{H}}$, the estimate can be given by

$$\hat{U}(k,l) = \frac{\bar{H}^*(k,l)V(k,l)}{\mid \bar{H}(k,l) \mid^2 + \gamma \mid Q(k,l) \mid^2 - \beta} \tag{3.26}$$

Compared with the Eq. (3.9), this estimate has an extra parameter β introducing the effect of the uncertainity in the PSF. However, β in Eq. (3.26) has a deregularization effect due to negative sign [9, 23].

In order to overcome the aforementioned deregularization effect, we modify the conventional constrained least-square problem by incorporating the statistical information about $\mathbf{N_1}$ and $\mathbf{n_2}$ in a different way. Notice that Eq. (3.13) can be written as

$$\mathbf{v} - \bar{\mathbf{H}}\mathbf{u} - \mathbf{N_1}\mathbf{u} = \mathbf{n_2}. \tag{3.27}$$

Given the estimate $\hat{\mathbf{u}}$ the perturbated residual vector ϵ can be defined as

$$\epsilon = \mathbf{v} - \bar{\mathbf{H}}\hat{\mathbf{u}} - \mathbf{N_1}\hat{\mathbf{u}}. \tag{3.28}$$

It is obvious that if $\hat{\mathbf{u}} = \mathbf{u}$ then $\epsilon = \mathbf{n_2}$. Since the perturbated residual vector and noise vector are random, it is reasonable to seek an estimate $\hat{\mathbf{u}}$ such that the average value of the squared-norm of the perturbated residual vector ϵ matches with that of the noise vector $\mathbf{n_2}$. Assuming all components of $\mathbf{n_2}$ are uncorrelated with zero mean and variance σ_2^2, it follows that

$$E[\| \mathbf{n_2} \|^2] = MN\sigma_2^2. \tag{3.29}$$

Hence, the conventional constrained least-squares problem can be stated as

Minimize $\| \mathbf{Q}\hat{\mathbf{u}} \|^2$

Subject to $E[\| \mathbf{v} - \bar{\mathbf{H}}\hat{\mathbf{u}} + \mathbf{N_1}\hat{\mathbf{u}} \|^2] = E[\| \mathbf{n_2} \|^2]$.

Assuming that the uncertainty matrix $\mathbf{N_1}$ has zero mean elements, the lefthand side of the constraint can be further simplified and the constraint becomes

$$\| \mathbf{v} - \bar{\mathbf{H}}\hat{\mathbf{u}} \|^2 + E[\| \mathbf{N_1}\hat{\mathbf{u}} \|^2]. \tag{3.30}$$

Now, Eqs. (3.19), (3.24) and (3.30) yield

$$E[\| \mathbf{n_2} \|^2] - \| \mathbf{u} \|^2 E[\| \mathbf{N_1} \|^2] \leq \| \mathbf{v} - \bar{\mathbf{H}}\hat{\mathbf{u}} \|^2 \leq E[\| \mathbf{n_2} \|^2] + \| \mathbf{u} \|^2 E[\| \mathbf{N_1} \|^2].$$

Thus, the lower and upper bounds of the residual vector $\mathbf{r}$ are determined. Since $\| \mathbf{v} - \bar{\mathbf{H}}\hat{\mathbf{u}} \|^2 \geq 0$, the proposed method can be applied if and only if the degraded images satisfy the requirement:

$$E[\| \mathbf{N_1} \|^2] \leq \frac{E[\| \mathbf{n_2} \|^2]}{\| \mathbf{u} \|^2}.$$

That was the reason why we chose $\sigma_1^2 = 0.0025$.

Returning to the optimization problem, a straightforward lagrangian minimization yields

$$\hat{\mathbf{u}} = (\bar{\mathbf{H}}^{\mathbf{T}}\bar{\mathbf{H}} + \gamma\mathbf{Q}^{\mathbf{T}}\mathbf{Q} + E[\mathbf{N_1^T N_1}])^{-1}\bar{\mathbf{H}}^{\mathbf{T}}\mathbf{V}. \tag{3.31}$$

Assume that all the elements of $\mathbf{N_1}$ are uncorrelated with variance σ_1^2. Eq. (3.31) can be further reduced to

$$\hat{\mathbf{u}} = (\bar{\mathbf{H}}^{\mathbf{T}}\bar{\mathbf{H}} + \gamma\mathbf{Q}^{\mathbf{T}}\mathbf{Q} + IJ\sigma_1^2\mathbf{I})^{-1}\bar{\mathbf{H}}^{\mathbf{T}}\mathbf{v} \tag{3.32}$$

where $\gamma = \frac{1}{\lambda}$ and λ is a lagrange multiplier. Comparing with the conventional constrained least-square filter [14], Eq. (3.31) has an additional term, $E[\mathbf{N_1^T N_1}]$, which accounts for the statistical characteristics of the perturbations in the PSF.

Since $\bar{\mathbf{H}}$, $\mathbf{N_1}$ and $\mathbf{Q}$ are block circulant matrices, the 2D-DFT can be applied and Eq. (3.32) can be written as

$$\hat{U}(k,l) = \frac{\bar{H}^*(k,l)V(k,l)}{\mid \bar{H}(k,l) \mid^2 + \gamma \mid Q(k,l) \mid^2 + IJ\sigma_1^2}. \tag{3.33}$$

From Eq. (3.28), the squared-norm of perturbated residual vector ϵ in the discrete frequency domain can be written as

$$\| \epsilon \|^2 = \frac{1}{MN} \sum_{k=0}^{M-1} \sum_{l=0}^{N-1} (\mid V(k,l) - H(k,l)\hat{U}(k,l) \mid^2 + IJ\sigma_1^2 \mid \hat{U}(k,l) \mid^2) \tag{3.34}$$

Using the Newton-Raphson method, given in the previous section, a γ that satisfies the constraint can be found iteratively. It can be shown [14] that $\| \epsilon \|$ is a monotonic function of γ, so that the algorithm yields a unique γ. The algorithm of the proposed method can be summarized as follows:

1. Choose an initial value of γ.

2. Compute $\hat{U}(k,l)$ using Eq. (3.33).

3. Compute $\| \epsilon \|^2$ using Eq. (3.34).

4. While $\| \| \epsilon \|^2 - \| \mathbf{n_2} \|^2 | \geq ftol$; if $\| \epsilon \|^2 - \| \mathbf{n_2} \|^2 > 0$ reduce γ else increase γ. Go to step 3.

5. Stop iteration.

Where *ftol* in step four determines the accuracy of the constraint. The convergence of the above algorithm was observed to be highly depended on the initial choice of γ.

Choosing $\mathbf{Q}$ as the second order difference operator, the proposed algorithm yields Fig. 3.13b and Fig. 3.14b as the restored form of images in Fig. 3.10. Fig. 3.13b

Figure 3.13: Restoration of Fig. 3.10a when $\mathbf{Q}$ is second order difference operator: (a) Conventional constrained least-squares; $AMSE = 577.980$, $\gamma = 1.776$ at 6 iterations, (b) The proposed method: $AMSE = 516.840$, $\gamma = 0.18331$ at 5 iterations

is obtained when $\| \mathbf{n_2} \|^2$ is 3000000 with tolerance 1000 and the initial value of γ is 0.001 with tolerance 1.0E-6. Similarly, Fig. 3.14b is obtained when $\| \mathbf{n_2} \|^2$ is 2000000 with tolerance 1000 and the initial value of γ is 0.001 with tolerance 1.0E-6. For the purpose of comparison, we also applied the conventional second order difference filter (Eq. 3.9) to images in Fig. 3.10 yielding Fig. 3.13a and Fig. 3.14a. Fig. 3.13a is obtained when $\| \mathbf{n_2} \|^2$ is 3000000 with tolerance 1000 and the initial value of γ is 0.01 with tolerance 1.0E-6. Similarly, Fig. 3.14a is obtained when $\| \mathbf{n_2} \|^2$ is 2000000 with tolerance 1000 and the initial value of γ is 0.01 with tolerance 1.0E-6.

Hence, compared with the conventional least-squares filter, inverse filter and Wiener filter, the proposed method may improve both the quality and AMSE of the restorations depending on the images to be restored.

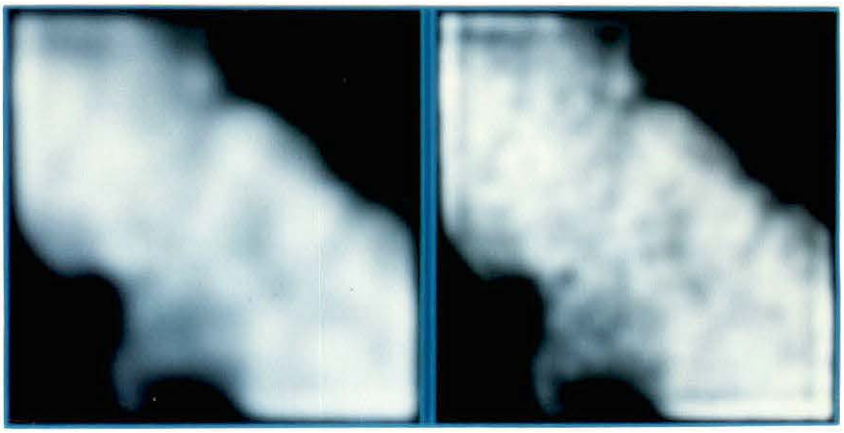

Figure 3.14: Restoration of Fig. 3.10b when $\mathbf{Q}$ is second order difference operator: (a) Conventional constrained least-squares; $AMSE = 311.943$, $\gamma = 2.47$ at 6 iterations. (b) The proposed method; $AMSE = 290.749$, $\gamma = 0.133$ at 5 iterations

Restoration of Noisy Images Blurred by Unknown PSF

In many practical applications, the PSF of an imaging system is usually unknown. Most of the existing restoration schemes were developed under the assumption that the PSF is known. In this section, we attempt to measure the PSF of an X-ray imaging system in an appropriate way before pseudoinverse restoration technique is applied.

For an imaging system which is a linear shift invariant system, the PSF can be defined as the image in the image plane due to an ideal source at the origin in the object plane. Using this definition, the PSF of the X-ray imaging system is approximately determined.

The X-ray imaging system that we dealt with has good resolution and very little blurring effect. For an introduction of blurring effect that a normal eye can easily realize, the distance between the film and X-ray source was kept about 120 cm and the object *phalanges* was located 20 cm away from the film towards the X-ray source. Also a few small spherically shaped metal pieces were placed in the same plane as the object. Here we assumed that these small metal parts would act like ideal sources in the spatial domain and that the amplification factor of system is negligible due to the relatively large distance between the source and the object. Fig. 3.2 shows an image captured under the above conditions. As seen in Fig.3.2, the captured image of phalanges has moderate degree of blur, and the images of spherical metal pieces are enlarged to some extent. For the purpose of restoration, any one of these points is taken as the estimate of the PSF of the imaging system. Isolating one of these points in Fig.3.2-b, the PSF of the system was captured in an array of size of 25x25. Next,

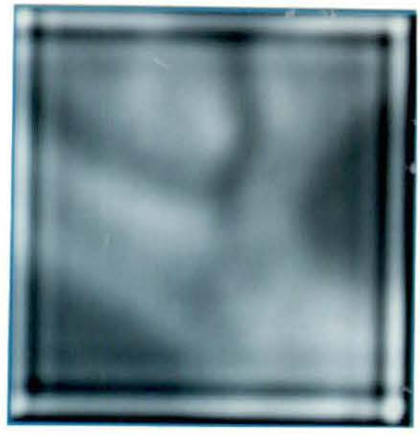

Figure 3.15: Restoration of image in Fig. 3.2a by Pseudoinverse filter; $\gamma = 0.049$ at 4 iterations

program MAIN2 read and normalized the PSF and applied pseudoinverse filtering technique. The noise variance required for the pseudoinverse filtering routine was measured as $\sigma^2 = 17.486$. Hence, the restored form of Fig. 3.2-a is given in Fig. 3.15 when $\| \mathbf{n} \|^2$ is 5000000 with tolerance 1000 and the initial value of γ is 0.01 with tolerance 1.0E-6. As seen in Fig. 3.15, the blurring effect is reduced but the wrap-around and end effects are introduced in the restoration process. However, the quality of Fig. 3.15 is obviously better than that of Fig. 3.2-a.

CHAPTER 4. TOTAL LEAST SQUARES

Total Least Squares (TLS) is a method of solving the system of equations $\mathbf{v} = \mathbf{Hu}$ when the vector $\mathbf{v}$ and the matrix $\mathbf{H}$ are both corrupted by noise [8, 9, 10]. It is different from conventional least squares (LS) that only accounts for errors in $\mathbf{v}$. For fitting a line to the points in a plane, the TLS finds a solution in the sense of minimizing the sum of the squared perpendicular distance; however, LS minimizes the vertical distance [9].

In the literature, Silvia and Tacker [21] applied the TLS approach to the inverse scattering problem to infer the shape, size and structural properties of an object from scattering measurements which result from seismic, acoustic or electromagnetic probes. Next, Rahman and Yu [19] used the TLS to improve the resolution of the closely spaced frequencies of multiple sinusoids when the signal to noise ratio of the received signal is low. They found that TLS yielded better frequency estimates than the principal eigenvector method in resolving both damped and undamped sinusoids in terms of average square error and bias. Abatzoglou and Mendel [1] introduced constrained total least squares by considering the noise perturbations of $\mathbf{v}$ and $\mathbf{H}$ to be linear functions of a common noise source vector.

Mathematical Derivation of TLS

In the conventional least-squares problem (LS), we are given a set of linear equations

$$\mathbf{Ax} = \mathbf{b} + \mathbf{r} \tag{4.1}$$

where $\mathbf{A}$ is a data matrix of size mxn, $\mathbf{b}$ is an obsevation vector of size mx1 and $\mathbf{r}$ is the measurement error in $\mathbf{b}$. The solution, minimizing $\| \mathbf{b} - \mathbf{Ax} \|^2$ with respect to $\mathbf{x}$, is given by [10, 16, 23]

$$\mathbf{x_{LS}} = (\mathbf{A^T A})^{-1} \mathbf{A^T b}.$$

However, when the data matrix has additional error component $\mathbf{E}$, Eq. (4.1) can be written as

$$(\mathbf{A} + \mathbf{E})\mathbf{x} = \mathbf{b} + \mathbf{r}. \tag{4.2}$$

Therefore, the TLS problem was stated as [8, 9, 10, 13]

Minimize $\| \mathbf{E} \mid \mathbf{r} \|_F^2$

Subject to $(\mathbf{b} + \mathbf{r}) \epsilon Range \epsilon (\mathbf{A} + \mathbf{E})$

where $\| \cdot \|_F$ denotes the Frobenius norm, viz

$$\| \mathbf{G} \|_F^2 = \sum_i \sum_j g_{ij}^2.$$

In [8], the TLS problem was solved by the lagrange multipliers method and later in[9], it was solved by the singular value decomposition approach. In the following, the first approach will be given. Rewrite Eq. (4.2) as

$$([\mathbf{A} \mid \mathbf{b}] + [\mathbf{E} \mid \mathbf{r}]) \begin{bmatrix} \mathbf{x} \\ -1 \end{bmatrix} = \mathbf{0} \tag{4.3}$$

or

$$\mathbf{By} + \mathbf{Fy} = \mathbf{0} \tag{4.4}$$

where

$$\mathbf{B} = [\mathbf{A} \mid \mathbf{b}], \mathbf{F} = [\mathbf{E} \mid \mathbf{r}] \text{ and } \mathbf{y} = \begin{bmatrix} \mathbf{x} \\ -1 \end{bmatrix}. \tag{4.5}$$

The TLS problem can be restated as

Minimize $\| \mathbf{F} \|_F^2$

Subject to $(\mathbf{B} + \mathbf{F})\mathbf{y} = \mathbf{0}$

Using the lagrange multipliers method, the problem becomes

Minimize $Tr[\mathbf{F_T F}] - \underline{\lambda}^T(\mathbf{B} + \mathbf{F})\mathbf{y}$

where $\underline{\lambda}$ is the lagrange parameter vector. Taking the derivative of this function with respect to $\mathbf{F}$ and using the facts;

$$\frac{\partial \underline{\lambda}^{\mathbf{T}} \mathbf{Fy}}{\partial \mathbf{F}} = \underline{\lambda}\mathbf{y}^{\mathbf{T}} \tag{4.6}$$

and

$$\frac{\partial Tr[\mathbf{F}^{\mathbf{T}}\mathbf{F}]}{\partial \mathbf{F}} = 2\mathbf{F} \tag{4.7}$$

a stationary point can be given by

$$\mathbf{F_0} = \frac{1}{2}\underline{\lambda}\mathbf{y}^{\mathbf{T}}.$$

Substituting $\mathbf{F_0}$ into Eq. (4.4), it follows that

$$\underline{\lambda} = 2\frac{\mathbf{By}}{\mathbf{y}^{\mathbf{T}}\mathbf{y}}$$

and, hence,

$$\mathbf{F_0} = \frac{\mathbf{B}\mathbf{y}\mathbf{y}^{\mathrm{T}}}{\mathbf{y}^{\mathrm{T}}\mathbf{y}}.$$

Thus

$$\| \mathbf{F_0} \|_F^2 = Tr[\mathbf{F_0}^{\mathrm{T}}\mathbf{F_0}] = \frac{\mathbf{y}^{\mathrm{T}}\mathbf{B}^{\mathrm{T}}\mathbf{B}\mathbf{y}}{\mathbf{y}^{\mathrm{T}}\mathbf{y}}. \tag{4.8}$$

Since $\| \mathbf{F} \|_F^2 =$ is minimum when $\hat{\mathbf{y}}$ is the eigenvector associated with the smallest eigenvalue of $\mathbf{B}^{\mathrm{T}}\mathbf{B}$, the solution of $\mathbf{x_{TLS}}$ can be found via the following procedure:

1. Form the singular value decomposition of $\mathbf{B}$

   $$\mathbf{B} = \mathbf{U}\sum\mathbf{V}^{\mathrm{T}}$$

   where

   $$\mathbf{U}^{\mathrm{T}}\mathbf{U} = \mathbf{I_m}, \mathbf{V}^{\mathrm{T}}\mathbf{V} = \mathbf{I_{n+1}}$$

   and the matrix $\sum$ is diagonal consisting of the singular values of $\mathbf{B}$.

2. Let $\mathbf{z}$ be the column vector of $\mathbf{V}$ associated with the smallest singular value σ_{n+1}, then

   $$\begin{bmatrix} \mathbf{x_{TLS}} \\ -1 \end{bmatrix} = \frac{-\mathbf{z}}{z_{n+1}}$$

where z_{n+1} is the last element in $\mathbf{z}$. Note that the solution will not be unique if σ_{n+1} is multiple. Also $\mathbf{x_{TLS}}$ does not exist if $z_{n+1} = 0$.

Furthermore, it is known that a solution to an ill-conditioned least squares problem can be obtained by ridge regression [16]. Golub [9] demonstrated that the total least squares problem is a deregularization procedure or inverse of the ridge regression. Hence this property causes the condition of the TLS problem to be always worse than the condition of the corresponding LS problem.

Application of TLS to Image Restoration

In this section, we focus on the restoration of images degraded by either horizontal or vertical linear motion blur. The effect of linear horizontal motion blur can be expressed by [15]

$$v(m,n) = \sum_{j=0}^{N-1} h(n-j)u(m,j) \tag{4.9}$$

for $m = 0, 1, 2, \ldots, M-1$. The above equation can be be written in vector-matrix form as

$$\mathbf{v_m} = \mathbf{H}\mathbf{u_m}$$

where $\mathbf{v_m}$ and $\mathbf{u_m}$ are the mth rows of $v(m,n)$ and $u(m,n)$, respectively. Therefore, linear blur in each row can be considered as one dimensional convolution process.

Examining Eq. (4.9) uncovers two problems related to image restoration. The first problem is the estimation of $u(m,n)$ for each m by the knowledge of $h(n)$ and $v(m,n)$. On the other hand, the second problem is the estimation of $h(n)$ by the knowledge of $v(m,n)$ and $u(m,n)$.

For the purpose of illustration of the first problem, one dimensional data of length N=32 in Fig.4.1 was blurred by a stochastic PSF. The stochastic PSF was obtained by adding zero mean, uncorrelated noise of variance $\sigma_1^2 = 0.0001$ to the normalized Gaussian shaped PSF with variance 1.0 and length 9. The resulting blurred data was further added to by zero mean, uncorrelated observation noise of variance $\sigma_2^2 = 0.0121$. Fig. 4.1 shows the noisy data blurred by the stochastic PSF and the noisy input data, separately. The aim was to estimate the original signal from the degraded data sequence. Applying the least-squares and total least squares methods, the AMSE values of the estimates for different σ_1 and σ_2 are given in Table 4.1. Table 4.1

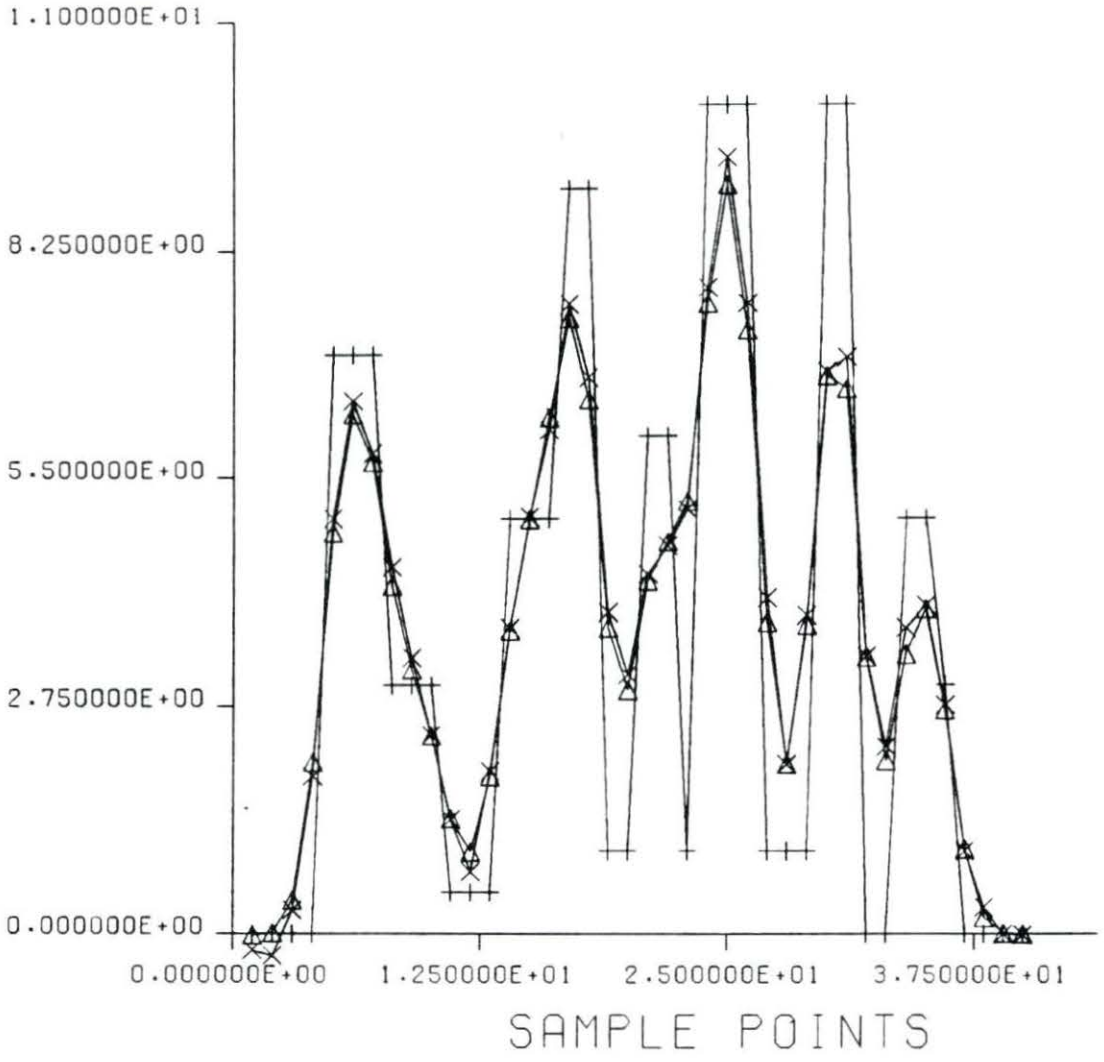

Figure 4.1: One dimensional simulation: +- Original data, X- Noisy data blurred by stochastic PSF, Δ- Noisy data to determine the PSF

shows that the TLS does not yield estimates closer to the original data than those of conventional least squares. This is because of the deregularization property of TLS. This property becomes significant when the problem is ill-conditioned. Even if the image is chosen parallel to the left singular vector of A associated with the smallest singular value (suggested by [26]), the LS solution performed better than the TLS solution for image restoration problems. As a result, TLS is not a good method in the estimation of the original image by the knowledge of the degraded noisy image and the stochastic PSF. However, TLS yielded promising results in dealing with the second problem. In this case, the vector matrix representation of Eq. (4.9) can be given as

$$\mathbf{v_m} = \mathbf{U}_\mathbf{m}^{'}\mathbf{h}^{'}$$

where $\mathbf{U}_\mathbf{m}^{'}$ is a toeplitz matrix and $\mathbf{h}^{'}$ is the unknown PSF vector. Here the input data is assumed to contain a zero mean uncorrelated noise component of variance $\sigma_1^2 = 0.0001$ inherently, and then this noisy input data is convolved with the deterministic part of the PSF used in the first problem. Next, the blurred data is further added to by zero mean uncorrelated observation noise of variance $\sigma_2^2 = 0.0121$. Table. 4.2 shows the AMSE values of LS and TLS simulations for a set of different σ_1 and σ_2. Examining this table for low values of σ_2 shows that TLS gave better results compared with those of LS. Finally, It can be concluded that TLS can be used confidently in estimating the PSF by knowing the degraded image and original image with noise.

Table 4.1: AMSE values of LS and TLS results in the estimation of Input Data

SNR	σ_1	σ_2	$AMSE_{LS}$	$AMSE_{TLS}$
20 db	0.01	0.3478	48.860	345.690
20 db	0.01	0.3478	59.331	196.165
30 db	0.01	0.11	3.714	31.906
30 db	0.001	0.11	5.651	8.394
30 db	0.0001	0.11	6.026	8.554
40 db	0.01	0.03478	1.250	1.960
40 db	0.001	0.03478	0.488	0.530
40 db	0.0001	0.03478	0.593	0.627
50 db	0.0001	0.011	0.056	0.057

Table 4.2: AMSE values of LS and TLS results in the estimation of PSF

SNR	σ_1	σ_2	$AMSE_{LS}$	$AMSE_{TLS}$
20 db	0.3478	0.1	57.318E-6	58.104E-6
20 db	0.3478	0.01	30.682E-6	30.330E-6
20 db	0.3478	0.001	31.272E-6	30.874E-6
30 db	0.11	0.1	36.316E-6	36.665E-6
30 db	0.11	0.01	3.168E-6	3.156E-6
30 db	0.11	0.001	3.108E-6	3.091E-6
40 db	0.03478	0.1	35.781E-6	36.078E-6
40 db	0.03478	0.01	0.573E-6	0.573E-6

CHAPTER 5. DISCUSSION

In this research, we dealt with various image restoration methods that have been implemented in the discrete frequency domain. The methods were tested on real images blurred by either deterministic or stochastic PSFs in the presence of signal-independent additive Gaussian white noise. Tables 5.1-5.2 list the AMSE values obtained from the restoration results in Chapter Three. Wiener filter simulations were performed under the assumption of zero mean and nonzero mean images, respectively. However, it is true that the real images have nonzero mean.

The major problem with image restoration methods is observed to be the edge effect due to the convolution wraparound at the borders of the restored images. The wrap-around is the result of the circular convolution process between the image to be restored and the restoration filter, when the size of the convolution exceeds the size of

Table 5.1: AMSE values of Restorations with deterministic PSF

Restoration Scheme: Deterministic PSF	Picture AMSE	X-ray Image AMSE
Inverse Filter	534.831	355.427
Wiener Filter (zero mean)	764.550	229.480
Wiener Filter (nonzero mean)	1192.276	3512.689
Pseudoinverse Filter	556.083	424.093
Constrained Least Squares Filter	499.829	265.089

Table 5.2: AMSE values of Restorations with stochastic PSF

Restoration Scheme: Stochastic PSF	Picture AMSE	X-ray Image AMSE
Wiener Filter (zero mean)	885.066	276.406
Wiener filter (nonzero mean)	1171.930	3516.431
Stochastic Wiener Filter (zero mean)	636.280	259.390
Stochastic Wiener F. (nonzero mean)	1149.934	3480.479
Second Order Diff. Operator	577.980	311.943
Proposed Algorithm	516.840	290.749

the DFT [2]. The restoration filters also introduced ringing effects at the borders of the restored images in the form of strip lines. The restoration process is a deblurring action or subtraction action as opposed to the convolution sum in blurring. Hence the restoration filters introduce negative PSF in the restoration and this causes the ringing in the regions of the image with sharp discontinuity such as at the borders [2].

The results of inverse filtering are shown in Fig. 3.5. Inverse filters are known to amplify noise during the restoration process and are extremely sensitive to SNR. However, inverse filter can perform well if there are no singularities in the PSF. In order to eliminate these shortcomings, the estimated image in frequency domain was set to zero whenever the 2D-DFT of the PSF is less than a suitably chosen threshold level.

The Wiener filter assumes a stationary random process and a linear estimation model. Fig. 3.6 demonstrates the results of Wiener filter restoration. The Wiener filter eliminates the ill-conditioned nature of the problem which is significant in inverse filtering. It necessitates the information about the power spectra of the original image and the noise process. It is this information that prevents the Wiener filter from being

unstable when the spectrum of the PSF approaches zero as happens in many real imaging systems. It can be seen from Eq. (3.6) that the Wiener filter becomes inverse filter as the spectrum of the noise process approaches to zero and it becomes zero as the spectrum of the original image approaches to zero. Therefore, it controls the ill-conditioning of the restoration by incorparating the information about the spectra.

When the PSF of the imaging system is stochastic, the Wiener filter can be modified to include the a priori information about the PSF in the restoration process. From Eq. (3.18), this information appears as a regularization parameter in the denominator. Fig. (3.11) and Fig. (3.12) are the restored forms of images in Fig. 3.10 using a conventional Wiener filter (Eq. (3.6)) and a modified Wiener filter (Eq. (3.18)). A significant improvement in the smoothness can be made by the restorations implemented by Eq. (3.18).

To eliminate the necessity of the knowledge about the power spectra of the noise and the original image required in the Wiener filter, a constrained least-squares filter can be used for the purpose of obtaining smoothed images. It can result in different filters depending on the choice of the constrained linear operator. Two such filters were the pseudoinverse filter and the second order difference filter. The restoration results of these filters are shown in Fig. 3.7 and Fig. 3.8, respectively. Compared with the pseudoinverse filter, the second order difference filter yielded smoother images with lower AMSE values. Constrained least-square methods also improve the sharpness and AMSE values of the images, when compared with the results of the inverse filter and the Wiener filter.

For the case of a stochastic PSF, it is possible to include the statistical char-

acteristics of the PSF in the constrained least-squares filter. The proposed image restoration method (Eq. (3.33)) and the second order difference filter (Eq. (3.10)) yield Fig. 3.14 and Fig. 3.13 as the restored form of images in Fig. 3.10, respectively. The restored images of our proposed method are sharper and visually more pleasing. The restored standard test image has lower AMSE value, when compared with both the second order difference filter and the Wiener filter.

When the PSF function of the system is not known, it can be approximately determined by experimental calibration measurement. Fig. 3.2 represents a systematically blurred real image and dots from which the PSF of the real X-ray imaging system is to be determined. Using this PSF, the pseudoinverse filter yields Fig. 3.15. Although Fig. 3.15 contains a ringing effect around the edges, a significant improvement is obvious, when compared with Fig. 3.2.

A new image restoration approach using the TLS method has been investigated. The TLS can be applied to restore noisy images blurred by stochastic PSF, or to estimate the impulse response of the imaging system. Referring to Table 4.2, the TLS yields better results than the conventional least-squares in estimating the PSF for high values of SNR. However, for the image restoration problem that we dealt with, the TLS method yields estimates that are worse than those of the conventional least-squares method due to the deregularizing effect.

CHAPTER 6. CONCLUSION

In this thesis, the restoration of blurred images in the presence of additive signal-independent noise has been studied. Several restoration algorithms were discussed, implemented and compared.

We have implemented the inverse filter, the Wiener filter, the pseudoinverse filter and the second order difference filter to restore noisy images degraded by deterministic PSFs. Each method was observed to require some sort of a priori information. The Wiener filter requires the power spectra of the noise and the original image. Overall, the second order difference filter yielded smoother restored images with smaller AMSE values.

When the PSF is stochastic, the information about the uncertainty in the PSF, if available, should be incorporated in the restoration process to obtain better results. We have developed a method called stochastic constrained least-squares that can use this information. Furthermore, simulations show the effectiveness of the proposed algorithm.

Another way of restoring noisy images blurred by stochastic PSF is the use of the TLS. This method has a deregularization property that yields worse restored images than the conventional least-squares. However, the TLS yields better results in estimating the PSF of the imaging systems under specific conditions. From a

computational efficiency point of view, the frequency domain implementation of TLS may be possible and needs further development in the future.

In most of the practical applications, the PSF of the imaging systems is not available a priori and needs to be determined. Our attempt to determine the PSF of an X-ray imaging system by measurement has yielded promising results.

Finally, it should be emphasized that good restoration algorithms should be less sensitive to SNR, yield good resolution, and have a control ability over the restored images. They are also required to be computationally efficient and use less memory storage.

BIBLIOGRAPHY

[1] Abatzoglou, T. J. and J. M. Mendel. "Constrained total least squares." *IEEE 1987 ICASSP Proceedings*, 3 (Apr. 1987): 21485-21488.

[2] Andrews, H. C. and B. R. Hunt. *Digital Image Restoration*. Englewood Cliffs, NJ: Prentice-Hall, 1977.

[3] Biemond, J. "Stochastic Linear Image Restoration." In *Advances in Computer Vision and Image Processing*, T. S. Huang, Ed. vol. 2. London: JAI Press Inc., 1986.

[4] Combettes, P. L. and H. J. Trussell. "Methods for digital restoration of signals degraded by a stochastic impulse response." *IEEE Trans. Acoust. Speech, Signal Processing*, 37 (Mar. 1989): 393-401.

[5] Dudgeon, D. E. and R. M. Mersereau. *Multidimensional Digital Signal Processing*. Englewood Cliffs, NJ: Prentice-Hall, 1984.

[6] Frieden, B. R. "Image Enhancement and Restoration." In *Picture Processing and Digital Filtering*, T. S. Huang, Ed. New York: Springer, 1975.

[7] Gerald, C. F. and P. O. Patrick. *Applied Numerical Analysis*. Cambridge, Mass.: Addison Wesley Publishing Company, 1984.

[8] Golub, G. H. "Some modified matrix eigenvalue problems." *SIAM Rev.*, 15 (Apr. 1973): 318-334.

[9] Golub, G. H. and C. F. V. Loan. "An analysis of the total least squares problem." *SIAM J. Numer. Anal.*, 17 (Dec. 1980): 883-893.

[10] Golub, G. H. and C. F. V. Loan. *Matrix Computations*. Baltimore: Johns Hopkins University-Press, 1983.

[11] Guan, L. and R. K. Ward. "Restoration of randomly blurred images by the wiener filter." *IEEE Trans. Acoust. Speech, Signal Processing*, 37 (Apr. 1989): 589-592.

[12] Helstrom, C. W. "Image restoration by the method of least squares." *J. Opt. Soc. Am.*, 57 (Mar. 1967): 297-303.

[13] Huffel, S. V. and J. Vandewalle. "The Total Least Squares Technique: Computation, Properties and Applications." In *SVD and Signal Processing: Algorithms, Applications and Architectures*, F. Deprettere, Ed. New York: North Holland, 1988.

[14] Hunt, B. R. "The application of constrained least squares estimation to image restoration by digital computer." *IEEE Trans. Comput.*, C-22 (Sept. 1973): 805-812.

[15] Jain, A. K. *Fundamentals of Digital Image Processing.* Englewood Cliffs, NJ: Prentice Hall, 1989.

[16] Lawson, C. L. and R. J. Hanson. *Solving Least Squares Problems.* Englewood Cliffs, NJ: Prentice-Hall, 1974.

[17] Mascarenhas, N. D. A. and W. K. Pratt. "Digital image restoration under a regression model." *IEEE Trans. Cir. Sys.*, CAS-22 (Mar. 1975): 252-266.

[18] Pratt, W. K. *Digital Image Processing.* New York: Wiley, 1978.

[19] Rahman, M. A. and K. B. Yu. "Total least squares approach for frequency estimation using linear prediction." *IEEE Trans. Acoust. Speech, Signal Processing*, ASSP-35 (Oct. 1987): 1440-1454.

[20] Ross, G. "Iterative methods in information processing for object restoration." *Optica Acta*, 29 (1982): 1523-1542.

[21] Silvia, M. T. and E. C. Tacker. "Regularization of marchenko's integral equation by total least squares." *J. Acoust. Soc. Am.*, 72 (Oct. 1982): 1202-1207.

[22] Slepian, D. "Linear least squares filtering of distorted images." *J. Opt. Soc. Am.*, 57 (July 1967): 918-922.

[23] Stewart, G. W. *Introduction to Matrix Computations.* New York: Academic Press, 1973.

[24] Stockham, T. G., T. M. Cannon and R. B. Ingebretsen. "Blind deconvolution through digital signal processing." *Proc. IEEE*, 63 (Apr. 1975): 678-692.

[25] Trussell, H. J. and M. R. Civanlar. "The feasible solution in signal restoration." *IEEE Trans. Acoust. Speech, Signal Processing*, ASSP-32 (1984): 201-212.

[26] Vandewalle, P. and E. Deprettere. "A variety of Applications of Singular Value Decomposition in Identification and Signal Processing," In *SVD and Signal Processing: Algorithms, Applications and Architectures,* F. Deprettere, Ed. New York: North-Holland, 1988.

[27] Van Trees, H. L. *Detection, Estimation and Modulation Theory.* New York: John Wiley and Sons Inc., 1968.

[28] Ward, R. K. and B. E. A. Saleh. "Restoration of images distorted by systems of random impulse response." *J. Opt. Soc. Am.,* A2 (1985): 1254-1259.

[29] Ward, R. K. and B. E. A. Saleh. "Deblurring random blur." *IEEE Trans. Acoust. Speech, Signal Processing,* ASSP-35 (Oct. 1987): 1494-1498.

[30] Woods, J. W. and C. H. Radevan. "Kalman filtering in two dimensions." *IEEE Trans. Inform. Theory,* IT-23 (July 1977): 557-566.

[31] Youla, D. C. and H. Webb. "Image restoration by the method of convex projections: Part 1- Theory." *IEEE Trans. Med. Imaging,* MI-I (Oct. 1982): 81-94.

[32] Zhuang, X., E. Ostevold and R. M. Haralick. "The Principle of Maximum Entropy in Image Recovery." In *Image Recovery: Theory and Application,* H. Stark, Ed. New York: Academic Press, 1987.

ACKNOWLEDGEMENTS

I would like to express a special thank you to my major professor, Dr. Hsien-Sen Hung, whose expertise in signal processing and continuous advise in that field have led to the selection of this research topic.

I would like to thank Dr. William Brockman for being my co-major professor and, once again, Dr. David Carlson and Dr. Mufit Akinc for their enthusiasm and their interest to serve on my graduate commitee.

I would like to express my sincere gratitude to graduate students Ali R. Brown, Mathew Chackalackal and Scott Irwin for their help in digitizing the images, transferring the data and taking pictures from the computer screen.

And last, but not least, a very special word to my family members who once again stood patiently behind me, supported me and provided me with continuous encouragement throughout my educational career. My parents, Huseyin Kazim and Raziye: I thank you for being so close to me even though you were thousands of miles away.

APPENDIX

```
      PROGRAM MAIN1
C
C  This program generates images blurred by deterministic
C  or stochastic point spread function (PSF) in the
C  presence of additive noise.
C
C  y  is an integer image for input
C
C  yc & ycd are complex images degraded by deterministic
C           and stochastic PSF, respectively
C
C  h & hd are gaussian shaped deterministic and stochastic
C           PSF, respectively

      parameter(is=128,im=7)

C  is=2**im

      integer y(is,is)
      complex yc(is,is),uu,h(is,is),hd(is,is),ycd(is,is)
      character*32 outfile
      pi=4.0*atan(1.0)

C  Initialization

      do 10 j=1,is
      do 10 i=1,is
         y(i,j)=0
         yc(i,j)=cmplx(0.0,0.0)
```

```
      hd(i,j)=cmplx(0.0,0.0)
10    h(i,j)=cmplx(0.0,0.0)

C  PSF Generation

      mean=10
      var=4.0
      stdev=sqrt(var)
      sn=0.0
      iseed=27983
     do 20 j=1,2*mean-1
     do 20 i=1,2*mean-1
        t=float((i-mean)**2+(j-mean)**2)/(2.0*var)
        t=exp(-t)
        sn=sn+t
20    h(i,j)=cmplx(t,0.0)

C  Normalization of PSF h and generation of hd

     print *, 'ENTER variance of hd'
     read(5,*) psfv
     psfv=sqrt(psfv)
     do 30 j=1,2*mean-1
     do 30 i=1,2*mean-1
        h(i,j)=h(i,j)/sn

C  Mean and Variance of hd are h and psfv**2, respectively

      call normal(gdev,x2,iseed)
30    hd(i,j)=h(i,j)+cmplx(psfv*gdev,0.0)
     noise=0

C  Options to record h, hd in psf.dat and psfd.dat, respectively

C      outfile='psf.dat'
C      call arrange(h,is,is,outfile,3,noise)

C      outfile='psfd.dat'
C      call arrange(hd,is,is,outfile,4,noise)
```

```
C
C  Two dimensional discrete fourier trasform of size 128x128
C
       call fft(h,im,im,-1)
       call fft(hd,im,im,-1)
C
C  Correct the spatial domain shift because  h and hd are not
C  centered at the origin
C
       tz=2.0*pi*float(mean-1)/float(is)
       uu=cmplx(cos(tz),sin(tz))
      do 40 l=1,is
      do 40 k=1,is
         hd(k,l)=hd(k,l)*(uu**(k+l))
   40    h(k,l)=h(k,l)*(uu**(k+l))
C
C  Options to record DFT of h and hd
C      outfile='fpsf.dat'
C      call arrange(h,is,is,outfile,1,noise)

C      outfile='fpsfd.dat'
C      call arrange(hd,is,is,outfile,2,noise)
C
C  Read original image
      open(9,file='orim.dat',status='old')
      rewind(9)
      read(9,50) ix,iy

C  ix, iy are horizantal and vertical sizes of image

   50 format(2i5)
      if(ix.gt.is .or. iy.gt.is) then
      print *, 'ERROR => image is larger than 128x128'
      goto 1000
      endif
      read(9,51,end=60) ((y(i,j),j=1,ix),i=1,iy)
   51 format(16i5)

C  Conversion to complex image
```

```
   60 do 70 ik=1,ix
      do 70 il=1,iy
   70    yc(il,ik)=cmplx(float(y(il,ik)),0.0)
C
      call fft(yc,im,im,-1)
C
C  Multiply DFT's of original image and PSF's
C
      do 80 l=1,is
      do 80 k=1,is
         ycd(k,l)=yc(k,l)*hd(k,l)
   80    yc(k,l)=yc(k,l)*h(k,l)
C
C  Inverse DFT's
C
      call fft(yc,im,im,1)
      call fft(ycd,im,im,1)
C
C  Write  blurred images
C    deterministic PSF
      outfile='b.dat'
      call arrange(yc,ix,iy,outfile,2,noise)
C    stochastic PSF
      outfile='rb.dat'
      call arrange(ycd,ix,iy,outfile,7,noise)

C  write noisy and blurred images

      noise=1
C    deterministic PSF
      outfile='nb.dat'
      call arrange(yc,ix,iy,outfile,8,noise)
C    stochastic PSF
      outfile='nrb.dat'
      call arrange(ycd,ix,iy,outfile,4,noise)

 1000  print *
      end
```

```
      PROGRAM  MAIN2

C  This program implements:
C   1- Restoration in the presence of Deterministic PSF
C     a) Inverse Filtering
C     b) Wiener Filtering
C     c) Constrained Least Squares
C       - Second Order Difference
C       - Pseudoinverse Filtering
C   2- Restoration in the presence of Stochastic PSF
C     a) Modified Wiener Filtering
C     b) Modified Constrained Least Squares
C         - second order difference operator
C   3- Unknown PSF to be measured
C  in restoring blurred and noisy images
C
C  y - input image
C  yc - complex images in both spatial and frequency
C       domain
C  h  - Point Spread Function
C  q  - power spectrum in wiener filtering routine and
C       second order difference operator in
C       constrained least squares
C  x  - restored image
C  i,j - spatial domain variables
C  k,l - frequency domain variables

      parameter(is=128,im=7)

C  is=2**im

      integer y(is,is)
      complex yc(is,is),uu,h(is,is),thr,q(is,is),x(is,is)
      character*32 outfile
      character*32 infile
      pi=4.0*atan(1.0)
      p=sqrt(2.0*pi)
```

```
C  Initialization

      do 10 j=1,is
      do 10 i=1,is
         x(i,j)=cmplx(0.0,0.0)
         y(i,j)=0
         q(i,j)=cmplx(0.0,0.0)
         yc(i,j)=cmplx(0.0,0.0)
   10    h(i,j)=cmplx(0.0,0.0)

C  PSF Generation
  720 print *,'----PSF SELECTION----'
      print *
      print *,'1- Known PSF'
      print *,'2- Unkown PSF'
      print *,'3- None'
      print *
  730 print *,'   ENTER the selection 1,2 or 3 =>'
      read(5,*) isel
      go to (750,775,1000)isel
      go to 730
  750 print *,'----KNOWN PSF with GAUSSIAN SHAPE----'
      print *
      print *,'   ENTER  mean,variance of Gaussian Curve =>'
      read(5,*) mean,var
      print *,'wait'
      stdev=sqrt(var)
      sn=0.0
      do 20 j=1,2*mean-1
      do 20 i=1,2*mean-1
         t=float((i-mean)**2+(j-mean)**2)/(2.0*var)
         t=exp(-t)
         sn=sn+t
   20    h(i,j)=cmplx(t,0.0)

C  Normalization of PSF h

      do 30 j=1,2*mean-1
```

```
      do 30 i=1,2*mean-1
   30    h(i,j)=h(i,j)/sn
      ipsf=0
      go to 740
  775 print *,'----UNKNOWN PSF: Pseudoinverse Filtering'
      print *,'psf will be read from file psf.dat'
      open(12,file='psf.dat',status='old')
      read(12,60) ix2,iy2
      read(12,70,end=25) ((y(i,j),j=1,ix2),i=1,iy2)
   25 sn=0.0
      rewind(12)
      mean=int(ix2/2)
      do 26 j=1,ix2
      do 26 i=1,iy2
         sn=sn+float(y(i,j))
   26    h(i,j)=cmplx(float(y(i,j)),0.0)

C  Normalize the measured PSF

      do 27 j=1,ix2
      do 27 i=1,iy2
   27    h(i,j)=h(i,j)/sn
      ipsf=1

C  Calculate  DFT of PSF

  740 call fft(h,im,im,-1)

C  Correct the spatial domain shift because h is not
C  centered at the origin

      tz=2.0*pi*float(mean-1)/float(is)
      uu=cmplx(cos(tz),sin(tz))
      do 40 l=1,is
      do 40 k=1,is
   40    h(k,l)=h(k,l)*(uu**(k+l))
      print *, '   ENTER degraded image =>'

C  Read the image to be restored
```

```
      read(5,50) infile
   50 format(a32)
      open(9,file=infile,status='old')
      rewind(9)
      read(9,60) ix,iy
   60 format(2i5)
      if(ix.gt.is .or. iy.gt.is) then
      print *, 'ERROR => image is larger than 128x128'
      goto 1000
      endif
      read(9,70,end=80) ((y(i,j),j=1,ix),i=1,iy)
   70 format(16i5)
   80 do 90 ik=1,ix
      do 90 il=1,iy
   90    yc(il,ik)=cmplx(float(y(il,ik)),0.0)
      rewind(9)
      call fft(yc,im,im,-1)

C  Option to record DFT of image
C       outfile='ycfft.dat'
C       call arrange(yc,128,128,outfile,1,0)
      if(ipsf.eq.1) goto 834
  840 print *, '1- Restoration with Deterministic PSF'
      print *, '2- Restoration with Stochastic PSF'
      print *, '3- None'
      print *
  841 print *, '     ENTER the selection 1,2 or 3 =>'
      read(5,*) isel
      go to (800,900,1000)isel
      go to 841
  800 print *,'DETERMINISTIC PSF RESTORATION SCHEME'
      print *
      print *,' 1- Inverse Filtering'
      print *,' 2- Wiener Filtering'
      print *,' 3- Constrained Least Squares'
      print *,' 4- Quit'
      print *
      iflag=0
```

```
  801 print *,'      ENTER the selection 1,2,3 or 4 =>'
      read(5,*) isel
      go to (810,820,830,840)isel
      go to 801
  810 print *,'----INVERSE FILTERING----'
      print *
      print *,'      ENTER threshold level =>'
      read(5,*) tr
      do 100 l=1,is
      do 100 k=1,is
         t=h(k,l)*conjg(h(k,l))
       if (t.lt.tr) then
         x(k,l)=0.0
       else
         x(k,l)=yc(k,l)/h(k,l)
       endif
  100 continue
      call fft(x,im,im,1)
      print *,'ENTER the outfile =>'
      read(5,50) outfile
      call arrange(x,ix,iy,outfile,2,0)
      print *,' Routine is DONE'
      goto 800
  820 print *,'----WIENER FILTER----'
      print *,'wait'
C  read the original image to find spectrum

      open(8,file='orim.dat',status='old')
      rewind(8)
      read(8,60) ix1,iy1
      read(8,70,end=110) ((y(i,j),j=1,ix1),i=1,iy1)

C  Calculate the mean of the original image

      yav=0.0
      do 118 j=1,ix1
      do 118 i=1,iy1
  118 yav=yav+float(y(i,j))
      yav=yav/float(ix1*iy1)
```

```
  110 do 120 j=1,ix1
      do 120 i=1,iy1
         q(i,j)=cmplx(float(y(i,j))-yav,0.0)
         x(i,j)=cmplx(yav,0.0)
  120    y(i,j)=0
      call fft(q,im,im,-1)
      call fft(x,im,im,-1)

C  Subtract mean of the image from noisy image

      do 123 l=1,is
      do 123 k=1,is
  123 yc(k,l)=yc(k,l)-h(k,l)*x(k,l)

C  Enter white noise variance  measured either from
C  the degraded image or known a priori

      print *, 'ENTER Noise Variance => '
      read(5,*) var

C  iflag=1 if wiener filtering routine is called from
C  stochastic PSF restoration, hence the variance of
C  PSF should be included in the routine

      if(iflag.eq.1) then
      print *,'ENTER the variance of PSF =>'
      read(5,*) psfv

C  Multiply the variance of PSF by the size of PSF

      psfv=((float(2*mean-1))**2)*psfv
      else
      psfv=0.0
      endif
      do 130 l=1,is
      do 130 k=1,is
         eps=h(k,l)*conjg(h(k,l))

C  Cu - power spectrum of the original image
```

```
C  Also multiply the noise variance by is*is
C  because of PARSEVAL THEOREM

         Cu=q(k,l)*conjg(q(k,l))
         qr=var*float(is**2)/Cu
         x(k,l)=yc(k,l)*conjg(h(k,l))/(eps+psfv+qr)
  130    q(k,l)=cmplx(0.0,0.0)
      call fft(x,im,im,1)

C  Add the average to the restored image

      do 131 j=1,ix1
      do 131 i=1,iy1
  131 x(i,j)=x(i,j)+cmplx(yav,0.0)
      print *,'ENTER the outfile =>'
      read(5,50) outfile
      call arrange(x,ix,iy,outfile,3,0)
      print *,'Routine is DONE'
      if(iflag.eq.1) goto 900
      go to 800
  830 print *,'----CONSTRAINED LEAST SQUARES----'
      print *
      print *,' 1- Pseudoinverse Filtering'
      print *,' 2- Second Order Difference'
      print *,' 3- None'
      print *
  831 print *,'     ENTER the selection 1,2 or 3 =>'
      read(5,*) isel
      go to (834,832,800)isel
      go to 831
  832 print *,'----SECOND ORDER DIFFERENCE----'
      print *
      print *,'wait'

C  Second difference matrix initialization

       q(1,1)=cmplx(0.0,0.0)
       q(1,2)=cmplx(1.0,0.0)
       q(1,3)=cmplx(0.0,0.0)
```

```
      q(2,1)=cmplx(1.0,0.0)
      q(2,2)=cmplx(-4.0,0.0)
      q(2,3)=cmplx(1.0,0.0)
      q(3,1)=cmplx(0.0,0.0)
      q(3,2)=cmplx(1.0,0.0)
      q(3,3)=cmplx(0.0,0.0)

C  Take DFT of second difference operator

      call fft(q,im,im,-1)

C  Correct the spatial domain shift because q is not
C  centered at the origin

      tp=2.0*pi/float(is)
      uu=cmplx(cos(tp),sin(tp))
      do 140 l=1,is
      do 140 k=1,is
  140    q(k,l)=q(k,l)*(uu**(k+l))

C  Option to record DFT of q

C       outfile='qfft.dat'
C       call arrange(q,is,is,outfile,10)

      if(iflag.eq.1) then
      print *,'ENTER the variance of PSF'
      read(5,*) psfv
      psfv=(float((2*mean-1)**2))*psfv
      else
      psfv=0.0
      endif

C ----- Newton Raphson root finding algorithm

      print *,'ENTER => bias,ftol,gamtol,gam,nlim'

C  bias - estimated norm of noise term
C  ftol - tolerance in the value of function
```

```
C         around the root
C  gamtol - tolerance of the increment in gamma
C  gam - initial value of gamma to be determined
C  nlim - maximum number of iterations

      read(5,*) bias,ftol,gamtol,gam,nlim
      do 150 iter=1,nlim

C  NOTE THAT: here PARSEVALS THEOREM is used
C  fer - summation of the magnitude square of residual
C        in frequency domain
C  dfer - derivative of fer wrt gam
C  thr  - residual in frequency domain

        fer=0.0
        dfer=0.0
      do 160 l=1,is
      do 160 k=1,is
         eps=h(k,l)*conjg(h(k,l))
         yeps=yc(k,l)*conjg(yc(k,l))
         qx=q(k,l)*conjg(q(k,l))
         qr=gam*qx
         dfer=2.0*qr*qx*eps*yeps/(eps+psfv+qr)**3+dfer
  160    fer=fer+((psfv+qr)**2+psfv*eps)*yeps/(eps+psfv+qr)**2
      fer=fer/float(is*is)
      fer=fer-bias
      dfer=dfer/float(is*is)

C  Convergence of the algorithm can be increased by
C  multiplying dfer by a suitably chosen constant

      dfer=dfer
      del=fer/dfer
     print *,'iter',iter,'gam',gam,'del',del,'fer',fer

C  Decision to continue the iteration

      if (abs(del).le.gamtol.or.abs(fer).le.ftol) goto 190
       gam=gam-del
```

```
  150  continue

C  Use the optimum gamma for second order difference
C  restoration

  190 do 200 l=1,is
      do 200 k=1,is
         eps=h(k,l)*conjg(h(k,l))
         qr=gam*q(k,l)*conjg(q(k,l))
         x(k,l)=(yc(k,l)*conjg(h(k,l)))/(eps+qr+psfv)
 200     q(k,l)=cmplx(0.0,0.0)
      call fft(x,im,im,1)
      print *,'ENTER the outfile =>'
      read(5,50) outfile
      call arrange(x,ix,iy,outfile,4,0)
      print *,'Routine is DONE'
      if(iflag.eq.1) goto 900
      go to 830
  834 print *,'----PSEUDOINVERSE RESTORATION----'
C
C  Using the same variables as above

      print *
      print *, 'ENTER => bias,ftol,gamtol,gam,nlim'
      read(5,*) bias,ftol,gamtol,gam,nlim
      do 205 iter=1,nlim
         fer=0.0
         dfer=0.0
       do 210 l=1,is
       do 210 k=1,is
          eps=h(k,l)*conjg(h(k,l))
          yeps=yc(k,l)*conjg(yc(k,l))
          thr=yc(k,l)*gam/(eps+gam)
          dfer=(2.0*gam*eps*yeps/(eps+gam)**3)+dfer
  210     fer=fer+thr*conjg(thr)
       fer=fer/float(is*is)
       fer=fer-bias
       dfer=dfer/float(is*is)
       del=fer/dfer
```

```
      print *, 'iter',iter,'gam',gam,'del',del,'fer',fer
      if (abs(del).le.gamtol.or.abs(fer).le.ftol) goto 220
       gam=gam-del
  205 continue
  220 do 230 l=1,is
      do 230 k=1,is
         eps=h(k,l)*conjg(h(k,l))
  230 x(k,l)=yc(k,l)*conjg(h(k,l))/(eps+gam)
      call fft(x,im,im,1)
      print *,'ENTER the outfile =>'
      read(5,50) outfile
      call arrange(x,ix,iy,outfile,7,0)
      print *,'Routine is DONE'
      if(ipsf.eq.1) goto 1000
      go to 830
  900 print *,'----STOCHASTIC PSF RESTORATION SCHEME----'
      print *
      print *,'1- Wiener Filter'
      print *,'2- Constrained Least Squares:'
      print *,'   Second Order Difference'
      print *,'3- Quit'
      print *
      iflag=1
  901 print *,'  ENTER the selection 1,2 or 3 =>'
      read(5,*)isel
      go to (820,832,840)isel
      go to 901
 1000 print *
      end
```

```
      SUBROUTINE FFT(x,mrow,mcol,k)

C  This subroutine calculates two dimensional discrete
C  Fourier transform and its inverse.
C  x    -The two dimensional complex array; representing
C        the input when subroutine is called and returns
C        DFT or IDFT
C  mrow-The row or vertical axis written as 2**mrow
C  mcol-The column or horizantal written as 2**mcol
C  k    -If k=-1 then DFT
C        if k= 1 then IDFT

      complex x(128,128),u,w,t

      n=2**mcol
      pi=4.0*atan(1.0)

      do 100 ii=1,2**mrow

      do 20 l=1,mcol
      le=2**(mcol+1-l)
      le1=le/2
      u=(1.0,0.0)
      w=cmplx(cos(pi/float(le1)),k*sin(pi/float(le1)))
      do 20 j=1,le1
      do 10 i=j,n,le
      ip=i+le1
      t=x(ii,i)+x(ii,ip)
      x(ii,ip)=(x(ii,i)-x(ii,ip))*u
   10 x(ii,i)=t
   20 u=u*w
      nv2=n/2
      nm1=n-1
      j=1

      do 30 i=1,nm1
      if(i.ge.j) goto 25
```

```
      t=x(ii,j)
      x(ii,j)=x(ii,i)
      x(ii,i)=t
   25 kk=nv2
   26 if(kk.ge.j) goto 30
      j=j-kk
      kk=kk/2
      goto 26
   30 j=j+kk
  100 continue

      n=2**mrow

      do 200 jj=1,2**mcol

      do 120 l=1,mrow
      le=2**(mrow+1-l)
      le1=le/2
      u=(1.0,0.0)
      w=cmplx(cos(pi/float(le1)),k*sin(pi/float(le1)))
      do 120 j=1,le1
      do 110 i=j,n,le
      ip=i+le1
      t=x(i,jj)+x(ip,jj)
      x(ip,jj)=(x(i,jj)-x(ip,jj))*u
  110 x(i,jj)=t
  120 u=u*w
      nv2=n/2
      nm1=n-1
      j=1
      do 130 i=1,nm1
      if(i.ge.j) goto 125
      t=x(j,jj)
      x(j,jj)=x(i,jj)
      x(i,jj)=t
  125 kk=nv2
  126 if(kk.ge.j) goto 130
      j=j-kk
      kk=kk/2
```

```
      goto 126
130   j=j+kk

      if (k.eq.-1) goto 50
      do 35 ll=1,n
 35   x(ll,jj)=x(ll,jj)/float(n*(2**mcol))

 50   ff=12
200   continue
      return
      end
```

```
      SUBROUTINE NORMAL(x1,x2,yy)

C  This subroutine generates uncorrelated zero mean
C  gaussian random numbers of unity variance
C    yy      - any number greater than zero, iseed
C    x1, x2 - random numbers

        integer yy
        real t,x1,x2
        call random(0.0,1.0,rando,yy)
        x1=sqrt(-2.*log(rando))
        call random(0.0,1.0,rando,yy)
      t=6.2831853072*rando
     x2=x1*sin(t)
     x1=x1*cos(t)
     return
      end

      subroutine random(a,b,rando,yy)
      integer yy,m
      real a,b,rando
      yy=16807*yy
     m=2**31-1
      yy=mod(yy,m)
     if (yy.lt.0) then
      yy=yy+m
     endif
     rando=(float(yy)/float(m))*(b-a)+a
     return
       end
```

```
      SUBROUTINE ARRANGE(ain,ih,iv,outfile,ip,noise)

C  This subroutine converts the complex array into
C  integer number for output
C   ain - complex image array
C   ih  - number of rows or horizantal size
C   iv  - number of columns or vertical size
C   outfile - name of file to be outputted
C   ip - unit number
C   noise - determine whether output will be noisy or not
C           noise=0  no noise
C           noise=1  uncorrelated gaussian noise is added
C                    to the output

      complex ain(128,128)
      integer adat(128,128)
      real aout(128,128),amax
      character*32 outfile

      amax=0.0
      do 750 j=1,ih
      do 750 i=1,iv
      aout(i,j)=sqrt(ain(i,j)*conjg(ain(i,j)))
      adat(i,j)=int(aout(i,j))
  750 if (aout(i,j).gt.amax) amax=aout(i,j)

C  Normalization option

C      do 755 j=1,ih
C      do 755 i=1,iv
C      tk=(aout(i,j)*255.0)/amax
C  755 adat(i,j)=int(tk)

C  Noise adding routine

      if(noise.eq.1) then
      iseed=10000
```

```
      do 760 j=1,ih
      do 760 i=1,iv
      call normal(gasdev,x2,iseed)

C  Standart deviation of noise is 10.0, hence variance
C  is 100.0

      it=10*gasdev
      adat(i,j)=adat(i,j)+it
  760 continue
      endif

      open(ip,file=outfile,status='new')
      write(ip,780) ih,iv
  780 format(2i5)
      print *, 'write is started'
      write(ip,785) ((adat(i,j),j=1,ih),i=1,iv)
  785 format(16i5)
      close(ip)

      return
      end
```